New aspects in the implementation of the quasi-static method for the solution of neutron diffusion problems in the framework of a nodal method

New aspects in the implementation of the quasi-static method for the solution of neutron diffusion problems in the framework of a nodal method

D. Caron, S. Dulla*, P. Ravetto*

Politecnico di Torino, Dipartimento Energia
Corso Duca degli Abruzzi, 24 - 10129 Torino (Italy)

Abstract

The ability to accurately model the dynamic behaviour of the neutron distribution in a nuclear system is a fundamental aspect of reactor design and safety assessment. Due to the heavy computational burden associated to the direct time inversion of the full model, the quasi-static method has become a standard approach to the numerical solution of the nuclear reactor dynamic equations on the full phase space. The present paper is opened by an introductory critical review of the basics of the quasi-static scheme for the general neutron kinetic problem. Afterwards, the implementation of the quasi-static method in the context of a three-dimensional nodal diffusion theory model in hexagonal-z geometry is described, including some peculiar aspects of the adjoint nodal equations and the explicit formulation of the quasi-static nodal equations. The presentation includes the discussion of different formulations of the quasi-static technique. The results presented illustrate the features of the various formulations, highlighting the corresponding advantages and drawbacks. An adaptive procedure for the selection of the time interval between shape recalculations is also presented, showing its usefulness in practical applications.

Keywords: Neutron multigroup diffusion, Nuclear reactor dynamics, Quasi-static method, Nodal method

1. Introduction

The design and safety assessment of the innovative nuclear systems proposed for future development requires the accurate simulation of the behaviour of the neutron distribution during typical operational and accidental conditions. As the time inversion of the full model is often impractical due to computational limitations or even unnecessary as a result of the characteristics of the physical processes, the quasi-static method initially proposed long ago (Henry, 1958) has emerged as a standard approach to the modelling of nuclear reactor dynamics on the full phase space.

*Corresponding author
Email address: sandra.dulla@polito.it (S. Dulla)

The present work is oriented towards the implementation of the quasi-static method in a nodal diffusion theory solver which comprises the neutronic module of a coupled neutronics/thermal-hydraulics reactor analysis code (Bonifetto et al., 2013b,a). Following a general review of the the theoretical basis of the quasi-static method and solution algorithms, a detailed description of the implementation of various formulations of the method in the framework of a nodal discretisation of the time-dependent multigroup diffusion equations is provided. The results presented demonstrate the behaviour, both in terms of accuracy and performance, of different variants of the quasi-static method with respect to the reference, full inversion method.

2. Theoretical basis of the quasi-static method

The theoretical basis of the quasi-static method of solution of the time-dependent neutronics problems is critically reviewed in the context of neutron transport theory. The problem is first posed in the framework of the proper mathematical equations which describe the relevant physical phenomena. Afterwards, the fundamental hypotheses of the quasi-static approach are stated, thereby permitting the derivation of the full system of kinetics equations to be solved by the quasi-static algorithm. Finally, the available methods of solution of these equations are discussed.

2.1. Problem setting

The time-dependent neutron transport equation and delayed neutron precursors balance equations for a stationary medium may be written as

$$\begin{cases} \dfrac{1}{v(E)}\dfrac{\partial}{\partial t}\phi(\mathbf{r},E,\mathbf{\Omega},t) = -\mathcal{L}(\mathbf{r},E,\mathbf{\Omega},t)\phi(\mathbf{r},E,\mathbf{\Omega},t) + \mathcal{M}_p(\mathbf{r},E,\mathbf{\Omega},t)\phi(\mathbf{r},E,\mathbf{\Omega},t) \\ \qquad + \displaystyle\sum_{i=1}^{R}\frac{\chi_i(\mathbf{r},E)}{4\pi}\lambda_i c_i(\mathbf{r},t) + S(\mathbf{r},E,\mathbf{\Omega},t), \\ \dfrac{\chi_i(\mathbf{r},E)}{4\pi}\dfrac{\partial}{\partial t}c_i(\mathbf{r},t) = \mathcal{M}_i(\mathbf{r},E,\mathbf{\Omega},t)\phi(\mathbf{r},E,\mathbf{\Omega},t) - \dfrac{\chi_i(\mathbf{r},E)}{4\pi}\lambda_i c_i(\mathbf{r},t), \qquad i=1,\dots,R, \end{cases} \tag{1}$$

and subject to appropriate initial and boundary conditions. In Eqs. (1), $\phi(\mathbf{r},E,\mathbf{\Omega},t)$ represents the time-dependent angular neutron flux, $c_i(\mathbf{r},t)$ is the time-dependent delayed neutron precursor concentration for delayed neutron precursor family i and the operators are defined by

$$\mathcal{L}(\mathbf{r},E,\mathbf{\Omega},t)\phi(\mathbf{r},E,\mathbf{\Omega},t) \equiv \mathbf{\Omega}\cdot\nabla\phi(\mathbf{r},E,\mathbf{\Omega},t) + \Sigma_t(\mathbf{r},E,t)\phi(\mathbf{r},E,\mathbf{\Omega},t) - \int dE' \oint d\Omega'\ \Sigma_s(\mathbf{r},E'\to E,\mathbf{\Omega}'\cdot\mathbf{\Omega},t)\phi(\mathbf{r},E',\mathbf{\Omega}',t), \tag{2a}$$

$$\mathcal{M}_p(\mathbf{r},E,\mathbf{\Omega},t)\phi(\mathbf{r},E,\mathbf{\Omega},t) \equiv (1-\beta)\frac{\chi_p(\mathbf{r},E)}{4\pi}\int dE' \oint d\Omega'\ \nu\Sigma_f(\mathbf{r},E',t)\phi(\mathbf{r},E',\mathbf{\Omega}',t), \tag{2b}$$

$$\mathcal{M}_i(\mathbf{r},E,\mathbf{\Omega},t)\phi(\mathbf{r},E,\mathbf{\Omega},t) \equiv \beta_i\frac{\chi_i(\mathbf{r},E)}{4\pi}\int dE' \oint d\Omega'\ \nu\Sigma_f(\mathbf{r},E',t)\phi(\mathbf{r},E',\mathbf{\Omega}',t). \tag{2c}$$

In these expressions, the operator $\mathcal{L}(\mathbf{r}, E, \mathbf{\Omega}, t)$ is the total reaction operator except for fission and $\mathcal{M}_p(\mathbf{r}, E, \mathbf{\Omega}, t)$ and $\mathcal{M}_i(\mathbf{r}, E, \mathbf{\Omega}, t)$ are the prompt and delayed fission operators, respectively. Similarly, the total fission operator is defined as

$$\mathcal{M}(\mathbf{r}, E, \mathbf{\Omega}, t)\phi(\mathbf{r}, E, \mathbf{\Omega}, t) \equiv \mathcal{M}_p(\mathbf{r}, E, \mathbf{\Omega}, t)\phi(\mathbf{r}, E, \mathbf{\Omega}, t) + \sum_{i=1}^{R} \mathcal{M}_i(\mathbf{r}, E, \mathbf{\Omega}, t)\phi(\mathbf{r}, E, \mathbf{\Omega}, t). \tag{3}$$

A reference system is defined as the initial, unperturbed steady-state configuration from which the transient is initiated. By taking all time derivatives in Eqs. (1) to be zero and by assuming that the delayed neutron precursors concentrations are in equilibrium with the steady-state neutron flux, the static neutron transport equation is obtained

$$-\mathcal{L}_0(\mathbf{r}, E, \mathbf{\Omega})\phi_0(\mathbf{r}, E, \mathbf{\Omega}) + \mathcal{M}_0(\mathbf{r}, E, \mathbf{\Omega})\phi_0(\mathbf{r}, E, \mathbf{\Omega}) + S_0(\mathbf{r}, E, \mathbf{\Omega}) = 0, \tag{4}$$

where the subscript indicates the static, reference system. In addition to the solution of the direct equation of the reference system, it is possible to obtain the solution of the corresponding adjoint equation, the solution of which is physically significant as it represents the distribution of the neutron importance (Wigner, 1992; Ussachoff, 1956; Lewins, 1965). The adjoint of Eq. (4) is

$$-\mathcal{L}_0^\dagger(\mathbf{r}, E, \mathbf{\Omega})\phi_0^\dagger(\mathbf{r}, E, \mathbf{\Omega}) + \mathcal{M}_0^\dagger(\mathbf{r}, E, \mathbf{\Omega})\phi_0^\dagger(\mathbf{r}, E, \mathbf{\Omega}) + S_0^\dagger(\mathbf{r}, E, \mathbf{\Omega}) = 0, \tag{5}$$

where the dagger † represents an adjoint operator or an adjoint quantity. Both Eqs. (4) and (5) are accompanied by direct and adjoint boundary conditions, respectively.

2.2. The quasi-static method

The quasi-static method of solution of the time-dependent neutron balance equation and delayed neutron precursors balance equations (Henry, 1958; Ott and Meneley, 1969; Devooght and Mund, 1980) is based on the rationale that the neutron flux may be factorised into the product of two separate but correlated functions of the form

$$\phi(\mathbf{r}, E, \mathbf{\Omega}, t) \equiv T(t)\psi(\mathbf{r}, E, \mathbf{\Omega}, t), \tag{6}$$

where the amplitude function $T(t)$ depends only on time and the shape function $\psi(\mathbf{r}, E, \mathbf{\Omega}, t)$ depends on all of the phase space variables. The amplitude function, which is proportional to the magnitude of the total reactor power, is intended to follow the fastest evolving time scales while the shape function accounts for spatial and spectral variations whose temporal evolution occurs on a slower time scale. This assumption, combined with a suitable projection procedure, allows to separate the original system of partial differential equations for the neutron flux and the delayed neutron precursors concentrations, Eqs. (1), into two coupled systems of differential equations: a coupled set of ordinary differential equations for the amplitude and a coupled set of partial differential equations for the shape. The advantage of these operations is that it becomes possible to solve separately for the unknowns on their respective time scales,

potentially offering a significant reduction of computational effort based on the nature of the transient and the degree to which the system is coupled.

The mathematical formalism for the projection-separation procedure is as follows. The flux factorisation, Eq. (6), is rendered unique by imposing an initial condition on the amplitude function, $T(0) = 1$, and a normalisation condition (Henry, 1958) on the shape function

$$\left\langle \phi_0^\dagger(\mathbf{r}, E, \mathbf{\Omega}), \frac{1}{v(E)} \psi(\mathbf{r}, E, \mathbf{\Omega}, t) \right\rangle = \gamma(t) = \gamma_0, \qquad \forall t, \tag{7}$$

with γ_0 an arbitrary constant and the scalar product notation $\langle \cdot, \cdot \rangle$ denoting the integration over all independent phase space variables.

Substitution of the factorised form of the flux into Eqs. (1), projection of both onto the adjoint solution of the reference system, subtraction of Eq. (5) projected onto the solution of the direct problem from the first of the projected Eqs. (1) and the use of the normalisation condition allows to write the amplitude equations

$$\begin{cases} \dfrac{d}{dt} T(t) = \dfrac{\rho(t) - \widetilde{\beta}(t)}{\Lambda(t)} T(t) + \displaystyle\sum_{i=1}^{R} \lambda_i \widetilde{c}_i(t) + \widetilde{s}(t), \\ \dfrac{d}{dt} \widetilde{c}_i(t) = \dfrac{\widetilde{\beta}_i(t)}{\Lambda(t)} T(t) - \lambda_i \widetilde{c}_i(t), \quad i = 1, \ldots, R, \end{cases} \tag{8}$$

with the integral kinetics parameters given by the definitions

$$F(t) \equiv \left\langle \phi_0^\dagger(\mathbf{r}, E, \mathbf{\Omega}), \mathcal{M}(\mathbf{r}, E, \mathbf{\Omega}, t) \psi(\mathbf{r}, E, \mathbf{\Omega}, t) \right\rangle, \tag{9a}$$

$$\Lambda(t) \equiv \frac{1}{F(t)} \left\langle \phi_0^\dagger(\mathbf{r}, E, \mathbf{\Omega}), \frac{1}{v(E)} \psi(\mathbf{r}, E, \mathbf{\Omega}, t) \right\rangle, \tag{9b}$$

$$\widetilde{\beta}_i(t) \equiv \frac{1}{F(t)} \left\langle \phi_0^\dagger(\mathbf{r}, E, \mathbf{\Omega}), \mathcal{M}_i(\mathbf{r}, E, \mathbf{\Omega}, t) \psi(\mathbf{r}, E, \mathbf{\Omega}, t) \right\rangle, \tag{9c}$$

$$\begin{aligned} \rho(t) \equiv & \frac{1}{F(t)} \left\langle \phi_0^\dagger(\mathbf{r}, E, \mathbf{\Omega}), \left[-\delta\mathcal{L}(\mathbf{r}, E, \mathbf{\Omega}, t) + \delta\mathcal{M}(\mathbf{r}, E, \mathbf{\Omega}, t) \right] \psi(\mathbf{r}, E, \mathbf{\Omega}, t) \right\rangle \\ & - \frac{1}{F(t)} \left\langle S_0^\dagger(\mathbf{r}, E, \mathbf{\Omega}), \psi(\mathbf{r}, E, \mathbf{\Omega}, t) \right\rangle, \end{aligned} \tag{9d}$$

$$\widetilde{c}_i(t) \equiv \frac{1}{\Lambda(t) F(t)} \left\langle \phi_0^\dagger(\mathbf{r}, E, \mathbf{\Omega}), \frac{\chi_i(\mathbf{r}, E)}{4\pi} c_i(\mathbf{r}, t) \right\rangle, \tag{9e}$$

$$\widetilde{s}(t) \equiv \frac{1}{\Lambda(t) F(t)} \left\langle \phi_0^\dagger(\mathbf{r}, E, \mathbf{\Omega}), S(\mathbf{r}, E, \mathbf{\Omega}, t) \right\rangle, \tag{9f}$$

in which the delta notation δ indicates the absolute perturbation of an operator with respect to its value for the reference system.

In Eqs. (9), $\Lambda(t)$ is the effective neutron lifetime, $\widetilde{\beta}_i(t)$ is the effective delayed neutron fraction for delayed neutron precursor family i, $\rho(t)$ is the dynamic reactivity, $\widetilde{c}_i(t)$ is the effective delayed neutron precursor amplitude for delayed neutron precursor family i and $\widetilde{s}(t)$ is the effective independent neutron source strength. The division by $F(t)$, and thus the definition of $F(t)$ itself, is arbitrary, affecting only the magnitudes of the quantities $\Lambda(t)$, $\widetilde{\beta}_i(t)$ and $\rho(t)$, but not the

solution of the amplitude equations themselves. Defining $F(t)$ according to the present definition, which has the physical interpretation of the time-dependent total fission importance, leads to an expression for the dynamic reactivity which is comparable to the perturbation theory expression for the static reactivity.

The origin of the time dependence of these terms arises from the variation in time either of the operators or of the shape function. Hence, the quasi-static approach foresees the computation of the integral kinetics parameters based on a known value of the shape function, which itself is computed from the full inversion of Eqs. (1).

2.3. Multiple quasi-static approaches to the time integration of the neutron transport equation

The discretisation of the time domain is shown in Fig. 1. A multiscale approach is employed, comprised of three embedded time scales, which are, from largest to smallest: the shape time step Δt_φ, the reactivity time step Δt_ρ and the amplitude time step Δt_T, which respect the hierarchy $\Delta t_\varphi \geq \Delta t_\rho \geq \Delta t_T$. As implied by the symbolic notation, the shape time steps are intended to resolve variations of the shape that are typically precipitated by a significant modification of the characteristics of the physical system. The reactivity time steps are intended to account for variations of the integral kinetics parameters which result from perturbations of the operators that do not necessarily involve major distortions of the shape. Finally, the amplitude time steps are intended to integrate the kinetics equations over an interval in which the shape and the kinetics parameters exhibit minor variations but the amplitude is changing as a result of disequilibrium of the dynamic system.

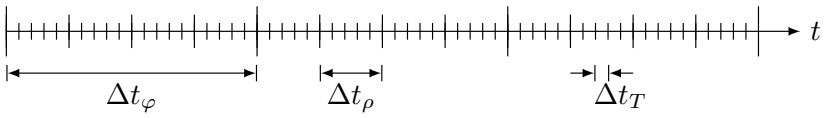

Figure 1: Multiscale time discretisation for quasi-static computations. Δt_φ: shape time step; Δt_ρ: reactivity time step; Δt_T: amplitude time step.

Various quasi-static algorithms exist for the integration of the neutron transport equation and the delayed neutron precursors balance equations in time; these approaches may be classified into two algorithmic categories on the basis of the quantities for which are solved at each of the various time steps. The first algorithmic category involves solving the set of equations for the amplitude and the shape while the second algorithmic category solves the set of equations for the amplitude and the flux. Both employ the same two fundamental sets of equations: the amplitude equations, Eqs. (8), and the time-dependent neutron transport equation with delayed neutron emissions, Eqs. (1). However, whereas the latter category can make direct use of Eqs. (1) to solve for the flux, the former requires their alteration in order to solve for the shape; the modification,

which results in the shape equations, may be written as

$$\begin{cases} \dfrac{1}{v(E)}\dfrac{\partial}{\partial t}\psi(\mathbf{r},E,\mathbf{\Omega},t) = -\left[\mathcal{L}(\mathbf{r},E,\mathbf{\Omega},t) + \dfrac{1}{v(E)}\dfrac{d}{dt}\log T(t)\right]\psi(\mathbf{r},E,\mathbf{\Omega},t) \\ \qquad + \mathcal{M}_p(\mathbf{r},E,\mathbf{\Omega},t)\psi(\mathbf{r},E,\mathbf{\Omega},t) + \dfrac{1}{T(t)}\left[\displaystyle\sum_{i=1}^{R}\frac{\chi_i(\mathbf{r},E)}{4\pi}\lambda_i c_i(\mathbf{r},t) + S(\mathbf{r},E,\mathbf{\Omega},t)\right], \\ \dfrac{\chi_i(\mathbf{r},E)}{4\pi}\dfrac{\partial}{\partial t}c_i(\mathbf{r},t) = T(t)\mathcal{M}_i(\mathbf{r},E,\mathbf{\Omega},t)\psi(\mathbf{r},E,\mathbf{\Omega},t) - \dfrac{\chi_i(\mathbf{r},E)}{4\pi}\lambda_i c_i(\mathbf{r},t), \qquad i=1,\ldots,R, \end{cases} \tag{10}$$

where the additional loss term results from the application of the product rule of differentiation to the factorised angular flux. If, instead of solving both sets of equations, the shape is assumed not to vary from the reference state and the only quantity for which is solved is the amplitude, the quasi-static method consistently reduces to the point kinetic (PK) method.

2.3.1. The improved quasi-static method

The improved quasi-static method (IQM) (Ott and Meneley, 1969) proposes to advance the flux across a shape time step through the simultaneous integration of the amplitude equations and the time-dependent shape equations across the shape time step. As a consequence of this choice of independent variables, the method requires a non-linear iterative approach due to the necessity to simultaneously solve for the shape and the amplitude such that the normalisation constraint of the shape is satisfied. The integration across a shape time step by means of IQM proceeds by integrating the amplitude equations to the end of the shape time step using integral kinetics parameters computed with the shape at the beginning of the shape time step followed by iteratively solving for the shape from Eqs. (10) until the normalisation condition is satisfied; within these iterations, the derivative of the amplitude is updated according to its definition in Eqs. (8) by recomputing the integral kinetics parameters with the shape function of the previous iteration on the normalisation condition.

The improved quasi-static method has evolved from the elaboration of the original quasi-static method (Ott and Madell, 1966), which disregards the time derivative of the shape function in Eqs. (10) with the justification that the time variation of the shape function is of lesser importance than that of the amplitude function. Both the original and the improved quasi-static methods may be considered to be improvements upon that which is now known as the adiabatic method (Henry, 1958), in which all time derivatives present in Eqs. (10) are neglected on the basis that the system reaches its new asymptotic configuration after only a few neutron lifetimes and thus may be described by the static balance equation of the perturbed system.

Another variant of the improved quasi-static method is that which may be referred to as the implicit improved quasi-static method (IIQM). Whereas IQM involves the integration of the amplitude equations across a shape time step using integral kinetics parameters which are computed explicitly with the shape at the beginning of the shape time step, IIQM involves their integration using integral kinetics parameters which are computed implicitly with the shape at the end of the shape time step. Consequently, the integration of the amplitude equations comprises part of the iterative procedure on the normalisation

condition used by IIQM. As a result, the shape, the amplitude and the derivative of the amplitude are all self-consistent, which is not necessarily true of IQM which, when more than one iteration on the normalisation condition is required, computes the amplitude using one set of integral kinetics parameters and the shape from another. Although IQM and IIQM may be expected to yield different results across a shape time step in which the shape undergoes significant variation, the two approaches become identical as the variations of the shape across a shape time step become negligible.

2.3.2. The predictor-corrector quasi-static method

The predictor-corrector quasi-static method (PCQM) (Kao and Henry, 1989) (although not referred to by this name until later (Dulla et al., 2008)) proposes to directly integrate the time-dependent flux equations across the shape time step and then apply the normalisation condition to acquire a shape. The shape thus obtained is employed in the determination of the integral kinetics parameters, consenting the successive integration of the amplitude equations to the end of the shape time step.

It has been shown that PCQM produces results of increased accuracy with respect to those of the improved quasi-static method for equal time steps, especially in the limit of large time steps (Dulla et al., 2008). This behaviour is attributed to two contributing factors. The first is the normalisation condition. For a given shape time step, IQM may or may not be capable of satisfying the normalisation condition to within decent accuracy, which contributes to a source of error that is absent from PCQM. The second is the shape itself used to compute the integral kinetic parameters. Namely, IQM employs the shape at the beginning of the time step, a quantity which is devoid of any information regarding the evolution during the time step, while the PCQM makes use of the shape at the end of the time step. While this disadvantage is mitigated by IIQM, normalisation remains an issue in IIQM, whereas in PCQM it does not.

Both in terms of algorithmic methodology and accuracy of results, PCQM is superior to IQM. Yet, in terms of computational performance, there are situations when PCQM may prove inferior to IQM. In particular, the computational effort associated with solving for the flux in PCQM instead of the shape in IQM becomes a drawback in divergent transients once the shape ceases to evolve, the reason for which is that the shape is free from amplitude effects while the flux is not. With the objective of addressing this deficiency, modifications to the basic procedure of PCQM have been proposed. In the modified predictor-corrector quasi-static method (MPCQM) (Dulla et al., 2008), the amplitude equations are preliminarily solved across the shape time step using integral kinetics parameters computed with the shape at the beginning of the shape time step (hence, in the same manner as IQM). The amplitude obtained from this calculation is then used to scale the flux at the beginning of the shape time step and thereby provide to the flux solver an initial guess which, to some extent, accounts for the variation in magnitude across the shape time step.

3. Implementation of the quasi-static method in the context of a nodal method

The implementation of the quasi-static method in the specific case of the neutron diffusion equations is now considered. The practical application of the

factorisation-projection technique to the nodal discretised form of the diffusion equations needs particular attention and the relevant details of the process are presented in the following. The starting point for the mathematical treatment is the multigroup, continuous space and time neutron diffusion model with delayed neutron emissions, which is obtained by applying the multigroup diffusion theory approximation to Eqs. (1).

3.1. Static and transient nodal equations of the direct problem

The reference multigroup equations are discretised in space according to a nodal approach. The scheme which is employed in the present work is inspired by the coarse mesh polynomial nodal method in hexagonal-z geometry proposed by Lawrence for implementation in the code DIF3D (Lawrence, 1983), which is extended to the transient multigroup neutron diffusion equations with a possible independent external source.

Following the application of these discretisation methods, the temporally continuous, spatially discrete transient multigroup neutron diffusion equations and delayed neutron precursors balance equations may be written in a general matrix form as

$$\begin{cases} \mathbb{V}^{-1}\dfrac{d}{dt}\overrightarrow{\mathbf{\Gamma}}(t) = \left[\mathbb{M}_p(t) - \mathbb{L}(t)\right]\overrightarrow{\mathbf{\Gamma}}(t) + \displaystyle\sum_{i=1}^{R}\lambda_i\overrightarrow{\mathbf{G}}_i(t) + \overrightarrow{\mathbf{S}}(t), \\ \dfrac{d}{dt}\overrightarrow{\mathbf{G}}_i(t) = \mathbb{M}_i(t)\overrightarrow{\mathbf{\Gamma}}(t) - \lambda_i\overrightarrow{\mathbf{G}}_i(t), \qquad i = 1,\ldots,R, \end{cases} \tag{11}$$

with the vectors and the matrix operators defined by

$$\overrightarrow{\mathbf{\Gamma}}(t) \equiv \begin{pmatrix} \mathbf{\Phi}(t) \\ \mathbf{J}^o(t) \\ \mathbf{J}^i(t) \end{pmatrix}, \tag{12a}$$

$$\overrightarrow{\mathbf{G}}_i(t) \equiv \begin{pmatrix} \mathbf{G}_i(t) \\ \mathbf{0} \\ \mathbf{0} \end{pmatrix}, \tag{12b}$$

$$\overrightarrow{\mathbf{S}}(t) \equiv \begin{pmatrix} \mathbf{S}(t) \\ \mathbf{0} \\ \mathbf{0} \end{pmatrix}, \tag{12c}$$

$$\mathbb{V}^{-1} \equiv \begin{pmatrix} \widehat{\mathbf{v}}^{-1} & \mathbf{0} & \mathbf{0} \\ \mathbf{0} & \mathbf{0} & \mathbf{0} \\ \mathbf{0} & \mathbf{0} & \mathbf{0} \end{pmatrix}, \tag{12d}$$

$$\mathbb{L}(t) \equiv \begin{pmatrix} \widehat{\mathbf{R}}(t) - \widehat{\mathbf{T}}(t) & \widehat{\mathbf{T}}_o(t) & -\widehat{\mathbf{T}}_i(t) \\ -\widehat{\mathbf{B}}(t) & \widehat{\mathbf{A}}(t) & -\widehat{\mathbf{C}}(t) \\ \mathbf{0} & -\widehat{\boldsymbol{\alpha}}(t) & \widehat{\mathbf{I}} \end{pmatrix}, \tag{12e}$$

$$\mathbb{M}_{p/i}(t) \equiv \begin{pmatrix} \widehat{\mathbf{F}}_{p/i}(t) & \mathbf{0} & \mathbf{0} \\ \mathbf{0} & \mathbf{0} & \mathbf{0} \\ \mathbf{0} & \mathbf{0} & \mathbf{0} \end{pmatrix}. \tag{12f}$$

Equations (11) represent, simultaneously for all nodes, all energy groups and all delayed neutron precursor families, neutron balance, Fick's law in terms of interface partial currents, continuity of interface partial currents and delayed neutron precursor balance for a stationary medium. In order to facilitate discussion, it is convenient to consider the unknowns present in these equations to adhere to a three-level structure: the first, outer level describes the discretisation in energy; the second, intermediate level describes the discretisation in space; and the third, inner level accounts for the mathematical approach of the spatial discretisation scheme. Accordingly, the structure may be interpreted as shown in Fig. 2 for the matrices (those which comprise $\mathbb{V}^{-1}$, $\mathbb{L}(t)$, $\mathbb{M}_p(t)$ and $\mathbb{M}_i(t)$) while the same interpretation may be applied to the vectors (those which comprise $\overrightarrow{\mathbf{\Gamma}}(t)$, $\overrightarrow{\mathbf{G}}_i(t)$ and $\overrightarrow{\mathbf{S}}(t)$) by assuming a degenerate second dimension.

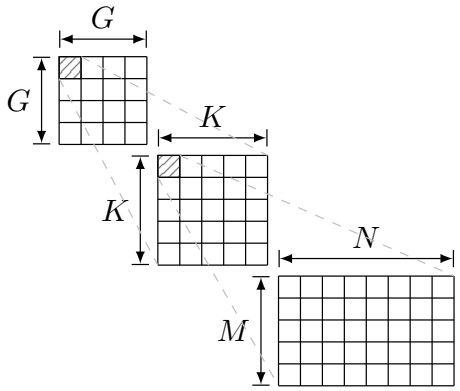

Figure 2: Structure of the matrices. G: total number of energy groups; K: total number of nodes; M,N: related to the mathematical scheme for the spatial discretisation.

The vectors $\mathbf{\Phi}(t)$, $\mathbf{J}^o(t)$ and $\mathbf{J}^i(t)$ contain the spatial moments of the neutron flux, the outgoing interface partial currents and the incoming interface partial currents, respectively, for each node and each neutron energy group. The vectors $\mathbf{G}_i(t)$ contain the spatial moments of the delayed neutron precursors emissivities divided by the decay constant for the delayed neutron precursor family i for each node and each neutron energy group, while the vector $\mathbf{S}(t)$ contains the spatial moments of the independent neutron source for each node and each neutron energy group.

The matrices $\widehat{\mathbf{R}}(t)$, $\widehat{\mathbf{T}}_o(t)$, $\widehat{\mathbf{T}}_i(t)$, $\widehat{\mathbf{A}}(t)$, $\widehat{\mathbf{B}}(t)$ and $\widehat{\mathbf{C}}(t)$ contain spatial coupling coefficients which depend on macroscopic removal cross sections, diffusion coefficients and node dimensions. As concerns their structures, all of the preceding matrices are diagonal in energy but have differing structures at the lower levels according to the geometry and the particularities of the nodal method in consideration. The matrices $\widehat{\mathbf{T}}(t)$, $\widehat{\mathbf{F}}_p(t)$ and $\widehat{\mathbf{F}}_i(t)$ contain the elements of the group-to-group scattering matrix (save for the in-group scattering component, which is embodied in $\widehat{\mathbf{R}}(t)$), the prompt neutron production matrix and the delayed neutron production matrix for the delayed neutron precursor family i,

respectively. These three matrices are all potentially full in energy but again have differing structures at the lower levels according to the geometry and the nodal approach.

The matrix $\widehat{\mathbf{v}}^{-1}$ is a strictly diagonal matrix which contains the inverses of the neutron group velocities. The matrix $\widehat{\boldsymbol{\alpha}}(t)$ is the superposition of an albedo matrix and a partial current permutation matrix. Therefore, the non-zero elements of $\widehat{\boldsymbol{\alpha}}(t)$ contain either albedo coefficients, which constitute boundary conditions at the external faces of the computational domain, or ones as necessary to guarantee the continuity of the interface partial currents of the adjacent nodes. The identity matrix is represented by $\widehat{\mathbf{I}}$.

In static form, the multigroup neutron diffusion equations reduce to

$$[\mathbb{M} - \mathbb{L}]\, \overrightarrow{\boldsymbol{\Gamma}} + \overrightarrow{\mathbf{S}} = \mathbf{0}, \tag{13}$$

with

$$\mathbb{M} \equiv \mathbb{M}_p + \sum_{i=1}^{R} \mathbb{M}_i. \tag{14}$$

These definitions are obtained by taking all time derivatives to be identically zero and by assuming that the delayed neutron precursors concentrations are in equilibrium with the static neutron flux distribution.

3.2. Adjoint nodal equations

Preliminary to the derivation of the adjoint nodal equations, it is necessary to define the scalar product, as its definition renders unique that of the adjoint operators. To this end, it is convenient to define the scalar product using a hybrid physical-mathematical approach

$$\left\langle \overrightarrow{\mathbf{v}}, \overrightarrow{\mathbf{u}} \right\rangle \equiv \overrightarrow{\mathbf{v}}^{T} \mathbb{A}\, \overrightarrow{\mathbf{u}}, \tag{15}$$

with $\overrightarrow{\mathbf{u}}$ and $\overrightarrow{\mathbf{v}}$ vectors in the same sense as $\overrightarrow{\boldsymbol{\Gamma}}$ and with the matrix $\mathbb{A}$ given by

$$\mathbb{A} \equiv \begin{pmatrix} \widehat{\mathbf{V}} & \mathbf{0} & \mathbf{0} \\ \mathbf{0} & \widehat{\mathbf{N}}_{\perp} & \mathbf{0} \\ \mathbf{0} & \mathbf{0} & \widehat{\mathbf{N}}_{\perp} \end{pmatrix}, \tag{16}$$

in which the matrices $\widehat{\mathbf{V}}$ and $\widehat{\mathbf{N}}_{\perp}$ are diagonal matrices whose non-zero elements are equal to the volumes and the transverse surface areas, respectively, of the nodes. Thus, the definition of the scalar product expressed by Eq. (15) is the discrete equivalent of an integral scalar product defined for continuous phase space variables.

For a reference configuration of the system, the adjoint nodal equations which describe the balance of neutron importance may be formulated as

$$\left[\mathbb{M}^{\dagger} - \mathbb{L}^{\dagger}\right] \overrightarrow{\boldsymbol{\Gamma}}^{\dagger} + \overrightarrow{\mathbf{S}}^{\dagger} = \mathbf{0}, \tag{17}$$

where the adjoint quantities are identified with a dagger. Starting from the definition of an adjoint operator, making use of the scalar product in Eq. (15)

and the diagonality of $\mathbb{A}$ to simplify notation, it is trivial to show that the matrix operators of the adjoint problem satisfy the criterion

$$\mathbb{H}^{\dagger} \equiv \mathbb{A}^{-1}\mathbb{H}^{T}\mathbb{A}, \tag{18}$$

with $\mathbb{H}$ an operator in the same sense as $\mathbb{M}$ or $\mathbb{L}$. Equation (18) is similar to the well known fact that the adjoint of a matrix is its conjugate transpose, which is simplified in the present case as the matrix operators of this particular problem are known to be defined only on the real portion of the complex plane. In general, $\mathbb{H}$ is not diagonal, hence the retention of the transpose notation and the inability to simplify the left multiplication by $\mathbb{A}^{-1}$ and the right multiplication by $\mathbb{A}$. Furthermore, this operation is necessary in order to correctly weight the off-diagonal elements of $\mathbb{H}$ when transposed, as this operation exchanges volume-averaged quantities (from the nodal balance equation) with surface-averaged quantities (from the Fick's law equation or the continuity equation).

For the problem in consideration, the adjoint matrix operators of the nodal balance equations, following several simplifications which are permitted by the structures of the matrices of the operators, are given by

$$\mathbb{L}^{\dagger} \equiv \begin{pmatrix} \widehat{\mathbf{R}} - \widehat{\mathbf{T}}^{T} & -\widehat{\mathbf{V}}^{-1}\widehat{\mathbf{B}}^{T}\widehat{\mathbf{N}}_{\perp} & \mathbf{0} \\ \widehat{\mathbf{N}}_{\perp}^{-1}\widehat{\mathbf{T}}_{o}^{T}\widehat{\mathbf{V}} & \widehat{\mathbf{A}}^{T} & -\widehat{\boldsymbol{\alpha}}^{T} \\ -\widehat{\mathbf{N}}_{\perp}^{-1}\widehat{\mathbf{T}}_{i}^{T}\widehat{\mathbf{V}} & -\widehat{\mathbf{C}}^{T} & \widehat{\mathbf{I}} \end{pmatrix}, \tag{19a}$$

$$\mathbb{M}^{\dagger} \equiv \begin{pmatrix} \widehat{\mathbf{F}}^{T} & \mathbf{0} & \mathbf{0} \\ \mathbf{0} & \mathbf{0} & \mathbf{0} \\ \mathbf{0} & \mathbf{0} & \mathbf{0} \end{pmatrix}. \tag{19b}$$

As regards the adjoint independent source vector, one faces the issue of correctly identifying, in physical terms, the adjoint of the independent source itself. Since the the adjoint independent source is not uniquely defined, the resulting adjoint solution differs on the basis of the definition of the adjoint independent source (Dulla et al., 2006). This situation is distinct from that of a critical system, for which the adjoint solution is unique for a given definition of the scalar product. As the purpose of this discussion is mathematical, it is taken for granted that the adjoint independent source vector is known or at the least can be determined in terms of known physical quantities.

The adjoint node-averaged flux and the adjoint outgoing and incoming surface-averaged interface partial currents which satisfy Eq. (17) with operators as in Eqs. (19) represent the solution of the adjoint problem. Equation (17) possesses several interesting characteristics that are not directly observed until the development of the response matrix equation to be used in the solution procedure.

The adjoint response matrix equation is obtained by first combining all of the individual equations of Eq. (17) to obtain

$$\widehat{\mathbf{A}}^{\dagger}\mathbf{J}^{o,\dagger} = \widehat{\mathbf{B}}^{\dagger}\mathbf{Q}^{\dagger} + \widehat{\boldsymbol{\alpha}}^{T}\widehat{\mathbf{C}}^{\dagger}\mathbf{J}^{o,\dagger}, \tag{20}$$

with

$$\widehat{\mathbf{A}}^{\dagger} \equiv \left[\widehat{\mathbf{A}} + \widehat{\mathbf{N}}_{\perp}\widehat{\mathbf{B}}\widehat{\mathbf{R}}^{-1}\widehat{\mathbf{T}}_{o}\widehat{\mathbf{N}}_{\perp}^{-1}\right]^{T}, \tag{21a}$$

$$\widehat{\mathbf{B}}^{\dagger} \equiv \left[\widehat{\mathbf{N}}_{\perp}^{-1}\left(\widehat{\boldsymbol{\alpha}}^{T}\widehat{\mathbf{T}}_{i}^{T} - \widehat{\mathbf{T}}_{o}^{T}\right)\widehat{\mathbf{V}}\widehat{\mathbf{R}}^{-1}\right], \tag{21b}$$

$$\widehat{\mathbf{C}}^{\dagger} \equiv \left[\widehat{\mathbf{C}} + \widehat{\mathbf{N}}_{\perp}\widehat{\mathbf{B}}\widehat{\mathbf{R}}^{-1}\widehat{\mathbf{T}}_{i}\widehat{\mathbf{N}}_{\perp}^{-1}\right]^{T}, \tag{21c}$$

$$\mathbf{Q}^{\dagger} \equiv \left[\widehat{\mathbf{F}} + \widehat{\mathbf{T}}\right]^{T}\boldsymbol{\Phi} + \mathbf{S}^{\dagger}. \tag{21d}$$

The final steps in the derivation of the adjoint response matrix equation include the partitioning of the off-diagonal blocks of the matrices $\widehat{\mathbf{A}}^{\dagger}$, $\widehat{\mathbf{B}}^{\dagger}$ and $\widehat{\mathbf{C}}^{\dagger}$ as well as the inversion of the block-diagonal component of $\widehat{\mathbf{A}}^{\dagger}$, thereby allowing to express the outgoing partial currents of a specific node in terms of an effective source and the incoming partial currents of that node. Such detail, however, is beyond the scope of the present discussion and furthermore is unnecessary as Eq. (20) is already abundant in information.

One interesting aspect of Eq. (20) is the matrix which multiplies the source term. The definition of $\widehat{\mathbf{B}}^{\dagger}$ does well to emphasise that the source of neutron importance of a particular node is due to the neutrons produced in adjacent nodes which arrive in the node itself reduced by the number of neutrons produced in the node itself which are ultimately transmitted to other nodes. Another interesting aspect of Eq. (20) is the implication which it has on the continuity of the adjoint partial current. The fact that the albedo matrix (even if in transposed form) does not multiply the adjoint outgoing partial current directly, but rather the quantity $\widehat{\mathbf{C}}^{\dagger}\mathbf{J}^{o,\dagger}$, implies that in the adjoint problem, the interface partial currents are discontinuous across nodal surfaces whereas the quantity $\widehat{\mathbf{C}}^{\dagger}\mathbf{J}^{o,\dagger}$ is continuous.

3.3. Quasi-static nodal equations

With the matrix operators and solution vectors as defined in Eqs. (12), it is possible to derive the quasi-static form of the nodal balance equations in a manner analogous to that earlier used with continuous phase space variables.

One begins with the factorisation of the flux, and consequently the current, into the product of an amplitude function and a normalised shape function

$$\overrightarrow{\boldsymbol{\Gamma}}(t) \equiv T(t)\overrightarrow{\boldsymbol{\Psi}}(t), \tag{22}$$

where $\overrightarrow{\boldsymbol{\Psi}}(t)$ is the shape of $\overrightarrow{\boldsymbol{\Gamma}}(t)$ and $T(t)$ is the amplitude defined such that $T(0) = 1$. It is clear that there is but one amplitude, common to both the flux and the partial currents, as the two quantities are directly proportional by Fick's law. The factorisation is rendered unique by imposing the normalisation condition

$$\left\langle \overrightarrow{\boldsymbol{\Gamma}}_{0}^{\dagger}, \mathbb{V}^{-1}\overrightarrow{\boldsymbol{\Psi}}(t)\right\rangle = \gamma_{0}, \qquad \forall t, \tag{23}$$

where $\overrightarrow{\boldsymbol{\Gamma}}_{0}^{\dagger}$ is the adjoint solution of the reference system and γ_0 is an arbitrary constant.

Substitution of the factorised form of the flux and current into Eqs. (11), projection of both onto the adjoint solution of the reference system, subtraction

of Eq. (17) projected onto the solution of the direct problem from the first of the projected Eqs. (11), use of the normalisation condition and finally the definition of a fission importance analogous to that of the steady-state system allows to write the amplitude equations, Eqs. (8), with the integral kinetics parameters given by

$$F(t) \equiv \left\langle \overrightarrow{\mathbf{\Gamma}}_0^\dagger, \mathbb{M}(t)\overrightarrow{\mathbf{\Psi}}(t) \right\rangle, \tag{24a}$$

$$\Lambda(t) \equiv \frac{1}{F(t)} \left\langle \overrightarrow{\mathbf{\Gamma}}_0^\dagger, \mathbb{V}^{-1}\overrightarrow{\mathbf{\Psi}}(t) \right\rangle, \tag{24b}$$

$$\widetilde{\beta}_i(t) \equiv \frac{1}{F(t)} \left\langle \overrightarrow{\mathbf{\Gamma}}_0^\dagger, \mathbb{M}_i(t)\overrightarrow{\mathbf{\Psi}}(t) \right\rangle, \tag{24c}$$

$$\rho(t) \equiv \frac{1}{F(t)} \left\langle \overrightarrow{\mathbf{\Gamma}}_0^\dagger, \left[\boldsymbol{\delta}\mathbb{M}(t) - \boldsymbol{\delta}\mathbb{L}(t)\right] \overrightarrow{\mathbf{\Psi}}(t) \right\rangle - \frac{1}{F(t)} \left\langle \overrightarrow{\mathbf{S}}_0^\dagger, \overrightarrow{\mathbf{\Psi}}(t) \right\rangle, \tag{24d}$$

$$\widetilde{c}_i(t) \equiv \frac{1}{\Lambda(t)F(t)} \left\langle \overrightarrow{\mathbf{\Gamma}}_0^\dagger, \overrightarrow{\mathbf{G}}_i(t) \right\rangle, \tag{24e}$$

$$\widetilde{s}(t) \equiv \frac{1}{\Lambda(t)F(t)} \left\langle \overrightarrow{\mathbf{\Gamma}}_0^\dagger, \overrightarrow{\mathbf{S}}(t) \right\rangle. \tag{24f}$$

The operators and sources of the pseudo-static fixed source problem to be solved either for the shape or for the flux are both obtained in a similar fashion once an approximation of the temporal variation of the spatial distribution of the delayed neutron precursors concentrations has been made. By assuming that the fission source per unit amplitude varies linearly across the shape time step, the delayed neutron precursors concentrations can be evaluated analytically according to the expression

$$\overrightarrow{\mathbf{G}}_i(t+\Delta t_\varphi) = \kappa_{0,i}\overrightarrow{\mathbf{G}}_i(t) + \frac{1}{\lambda_i}\left[\kappa_{1,i}\mathbb{M}_i(t)\overrightarrow{\mathbf{\Gamma}}(t) + \kappa_{2,i}\mathbb{M}_i(t+\Delta t_\varphi)\overrightarrow{\mathbf{\Gamma}}(t+\Delta t_\varphi)\right], \qquad i = 1, \ldots, R, \tag{25}$$

with

$$\kappa_{0,i} \equiv e^{-\lambda_i \Delta t_\varphi}, \tag{26a}$$

$$\kappa_{1,i} \equiv \frac{1}{\lambda_i \Delta t_\varphi}\left(1 - e^{-\lambda_i \Delta t_\varphi}\right) - e^{-\lambda_i \Delta t_\varphi}, \tag{26b}$$

$$\kappa_{2,i} \equiv 1 - \frac{1}{\lambda_i \Delta t_\varphi}\left(1 - e^{-\lambda_i \Delta t_\varphi}\right). \tag{26c}$$

The pseudo-static fixed source equation from which to solve for the shape in IQM is thus

$$\left[\mathbb{M}_{QS} - \mathbb{L}_{QS}\right] \overrightarrow{\mathbf{\Psi}}(t+\Delta t_\varphi) + \overrightarrow{\mathbf{S}}_{QS} = \mathbf{0}, \tag{27}$$

with

$$\mathbb{M}_{QS} \equiv \mathbb{M}_p(t+\Delta t_\varphi) + \sum_{i=1}^{R} \kappa_{2,i}\mathbb{M}_i(t+\Delta t_\varphi), \tag{28a}$$

$$\mathbb{L}_{QS} \equiv \mathbb{L}(t+\Delta t_\varphi) + \left[\frac{1}{\Delta t_\varphi} + \frac{d}{dt}\log T(t+\Delta t_\varphi)\right]\mathbb{V}^{-1}, \tag{28b}$$

$$\begin{aligned}\overrightarrow{\mathbf{S}}_{QS} \equiv & \left[\frac{1}{\Delta t_\varphi}\mathbb{V}^{-1} + \sum_{i=1}^{R}\kappa_{1,i}\mathbb{M}_i(t)\right]\overrightarrow{\mathbf{\Psi}}(t) \\ & + \frac{1}{T(t+\Delta t_\varphi)}\left[\sum_{i=1}^{R}\lambda_i\kappa_{0,i}\overrightarrow{\mathbf{G}}_i(t) + \overrightarrow{\mathbf{S}}(t+\Delta t_\varphi)\right],\end{aligned} \tag{28c}$$

while the pseudo-static fixed source equation of PCQM from which to solve for the flux is identical to that obtained for full inversion by the implicit, backward difference scheme

$$\left[\mathbb{M}_{QS} - \mathbb{L}_{QS}\right]\overrightarrow{\mathbf{\Gamma}}(t+\Delta t_\varphi) + \overrightarrow{\mathbf{S}}_{QS} = \mathbf{0}, \tag{29}$$

with

$$\mathbb{M}_{QS} \equiv \mathbb{M}_p(t+\Delta t_\varphi) + \sum_{i=1}^{R} \kappa_{2,i}\mathbb{M}_i(t+\Delta t_\varphi), \tag{30a}$$

$$\mathbb{L}_{QS} \equiv \mathbb{L}(t+\Delta t_\varphi) + \frac{1}{\Delta t_\varphi}\mathbb{V}^{-1}, \tag{30b}$$

$$\begin{aligned}\overrightarrow{\mathbf{S}}_{QS} \equiv & \left[\frac{1}{\Delta t_\varphi}\mathbb{V}^{-1} + \sum_{i=1}^{R}\kappa_{1,i}\mathbb{M}_i(t)\right]\overrightarrow{\mathbf{\Gamma}}(t) \\ & + \sum_{i=1}^{R}\lambda_i\kappa_{0,i}\overrightarrow{\mathbf{G}}_i(t) + \overrightarrow{\mathbf{S}}(t+\Delta t_\varphi).\end{aligned} \tag{30c}$$

3.4. Practical considerations

The integration of the shape (or the flux) equations and the amplitude equations across the shape time step, as well as the computation of the various derived quantities, is performed under the hypothesis that, in all dimensions of the phase space, the integral kinetics parameters, the fission source density per unit amplitude and the power density per unit amplitude vary linearly across the shape or reactivity time step.

Under the assumption that the shape varies linearly across the shape time step, the integral kinetics parameters are computed every reactivity time step using a shape function which is linearly interpolated across the shape time step and operators which are evaluated at the beginning and at the end of the reactivity time step. The actual values of the integral kinetics parameters that are used in the integration of the amplitude equations are their respective averages, obtained by assuming that each varies linearly across the reactivity time step. The amplitude equations are then solved exactly across the reactivity time step under the hypothesis that the integral kinetics parameters are constant on that same time step.

Within a shape time step, the spatial distribution of the delayed neutron precursors concentrations and the spatial distribution of the power are computed under the assumption that the fission source density per unit amplitude and the power density per unit amplitude, respectively, vary linearly across the reactivity time step, with their respective values at the beginning and at the end of the reactivity time step computed with a shape which is linearly interpolated across the shape time step. These assumptions are sufficient to ensure the continuity of the delayed neutron precursors concentrations (if normalisation were perfect) and of the power contemporaneously with the amplitude.

The preceding hypotheses are primarily intended for use with IIQM and PCQM, both of which have access to information about the shape at the end of the shape time step and therefore may make use of the assumed variation of the shape within the shape time step. Instead in IQM, the assumed variation of the shape is redundant as the integration of the amplitude equations is completed prior to the update of the shape function. Consequently, the delayed neutron precursors concentrations and the power density are discontinuous at the interface of successive shape time steps. While the delayed neutron precursors densities are intrinsically adjusted through their recomputation when the shape equations are solved, the power density is adjusted by imposing a continuity condition on the total power (Dulla et al., 2008), though at the cost of introducing a discontinuity on the amplitude.

3.5. Adaptive time integration procedure

In order to achieve maximum benefit from any of the quasi-static methods, it is expedient to introduce an appropriate algorithm for the adaptive control of the integration procedure. The principal objective of such an algorithm is the determination of the optimal shape time step for the current conditions of the transient, which may be either an expansion operation so as to avoid the unnecessary inversion of the full problem at times when variations of the shape, if any, are such that the system is insensitive to those changes, or a contraction operation so as to maintain a desired level of accuracy at times when variations of the shape are significant. This requires both appropriate metrics which are capable of indicating whether or not the shape undergoes a relevant and significant change as well as a practical algorithm which evaluates these metrics and employs them in the determination of new shape time steps.

An apposite indicator of the change in the shape function may take the form of a weighted vector norm of the difference in the shape vector between two points in time, normalised in order to permit a consistent comparison. As regards the nature of the norm itself, an L_2 vector norm is an appropriate measure of the magnitude of the weighted quantity. To this end, the indicator proposed for use in an adaptive quasi-static algorithm, henceforth refered to as the distortion of the shape function, is given by

$$\xi_\psi(t+\Delta t_\varphi) \equiv \frac{\left\| \mathbb{W}\left[\overrightarrow{\mathbf{\Psi}}(t+\Delta t_\varphi) - \overrightarrow{\mathbf{\Psi}}(t)\right]\right\|_2}{\frac{1}{2}\left\| \mathbb{W}\left[\overrightarrow{\mathbf{\Psi}}(t+\Delta t_\varphi) + \overrightarrow{\mathbf{\Psi}}(t)\right]\right\|_2}, \tag{31}$$

where $\mathbb{W}$ is a weight matrix and the notation $\|\cdot\|_2$ indicates the L_2 vector norm. For an absolute measure of the distortion, the weight matrix is simply the

identity matrix

$$\mathbb{W} \equiv \mathbb{I}, \tag{32}$$

while, for an importance-weighted measure of the distortion, the weight matrix takes the form

$$\mathbb{W} \equiv \mathrm{diag}\left(\overrightarrow{\mathbf{\Gamma}}_0^{\dagger}\right). \tag{33}$$

Although both of these weight functions (as well as others) are valid, the adjoint solution of the reference system is the logical choice, as it is mathematically consistent with the weight used to compute the inner products of the integral kinetics parameters and as it physically represents the neutron importance at each point in the phase space, thereby placing emphasis on changes at points of the phase space which are of significance to the solution.

The use of the parameter $\xi_\psi(t)$ in an adaptive time step selection algorithm is relatively straightforward. Consistent with the hypothesis that the shape varies linearly across the shape time step, it is possible to predict a maximum value for the shape time step over which the shape varies by a specified relative amount. This may be written as

$$\frac{\xi_\psi(t_{n-1})}{\Delta t_\varphi^{n-1}} = \frac{\xi_\psi^{\max}}{\Delta t_\varphi^{n}}, \tag{34}$$

with the index n introduced to differentiate among the different points in time and time steps and with $\xi_\psi^{\max}$ the maximum allowed relative distortion of the shape across a shape time step and is an input value. Thus, the maximum shape time step which respects Eq. (34) can be written in terms of known quantities.

In practice, the adaptive time step selection algorithm should take into consideration ancillary conditions other than merely the variation of the shape function. Based on historical experience (Meneley et al., 1967; Shober et al., 1978), some such factors may be cited as: an absolute maximum shape time step, a maximum multiple of the previous shape time step, a maximum relative variation of the amplitude across the shape time step and the intervention of a preset driving function. Each of these considerations can be used to suggest a value for the shape time step; the next shape time step is taken as the absolute minimum of all of the proposals. In the present approach, the solution computed to the end of the shape time step is accepted exclusively if each of the criteria evaluated to predict the shape time step is truly verified by the computed solution at the end of the shape time step; for IQM and IIQM, this includes the convergence criterion imposed on the normalisation condition.

Due to the latter requirement, the adaptive integration procedure requires further modification when either IQM or IIQM is employed. Precise details are omitted, however, in essence, the method further limits the expansion of the shape time step based on the normalisation condition error and its reduction behaviour at the previous shape time step. A strategy of this type is an arbitrary and, to some extent, conservative approach to the minimisation of the total number of times that the shape equations are be solved during the transient by attempting to minimise the probability of selecting a shape time step which leads to a situation in which the normalisation condition cannot be satisfied. A more desirable approach may be to maximise the ratio of the shape time step to the number of normalisation condition iterations required for that shape time step, a task which is difficult as the ratio is non-linear and depends on several factors.

4. Results

Results are presented for a transient applied to a small, non separable three-dimensional system. The quasi-static methods are first compared in terms of behaviour, accuracy and performance for a portion of the transient modelled using a constant shape time step. Subsequently, the adaptive time step selection procedure is enabled and the methods are once more assessed in terms of quality and performance.

The reactor under consideration is shown in Fig. 3 and consists of a central hexagonal assembly surrounded by three full concentric rings of assemblies. The axis is equipartitioned into two zones, with the lower and the upper zone each comprised of the same material pattern, but out of phase by a rotation of 180 degrees and inverted in the central assembly. The two materials, which are approximately representative of a light water reactor, are described by the two group diffusion theory parameters and the single delayed neutron precursor family provided in Table 1. Zero incoming partial current boundary conditions are imposed on all external surfaces of the system and the initial condition is critical. These specifications result in the initial distribution of the node-averaged flux and the node-averaged spectral ratio for selected assemblies which are shown in Figs. 4 and 5, respectively.

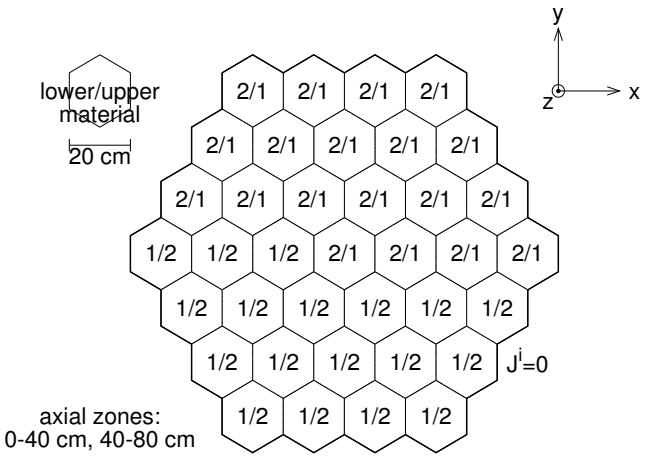

Figure 3: Initial configuration of the system studied for the transient. Labels of the form m_l/m_u indicate the material assigned to the lower (m_l) and upper (m_u) axial zone of each hexagonal assembly.

A compensated transient is initiated by instantaneously interchanging the materials (material 1 is substituted with material 2 and vice versa). While a configuration of this type is of course not feasible in an actual system, it does allow to consider a situation in which an initially critical system, after the transient initiator, retains its critical condition while it undergoes a strong

Table 1: Group constants used for the test calculations.

mat.	g	v_g [cm·s^{-1}]	D_g [cm]	Σ_{rg} [cm^{-1}]	Σ_{g1} [cm^{-1}]	$\nu\Sigma_{fg}$ [cm^{-1}]	χ_g [-]	χ_{g1} [-] [a]
1	1	1.000e+07	1.500	0.026	–	0.010	1.000	0.950
1	2	3.000e+05	0.500	0.180	0.015	0.200	0.000	0.050
2	1	1.000e+07	1.000	0.020	–	0.005	1.000	0.950
2	2	3.000e+05	0.500	0.080	0.010	0.099	0.000	0.050

a: $R = 1$ with $\lambda_1 = 0.08$ s^{-1} and $\beta_1 = 0.00750$.

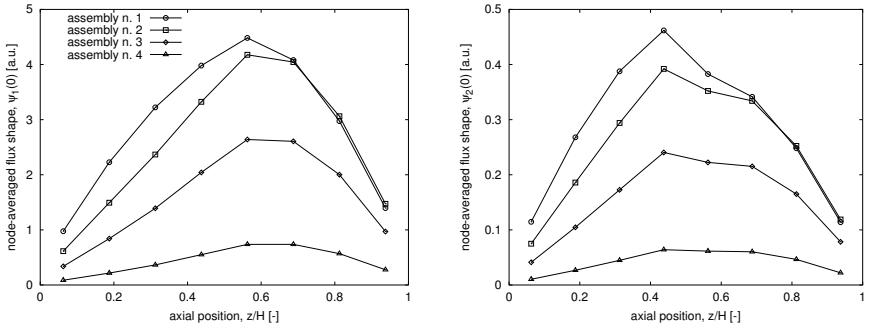

Figure 4: Initial axial distribution of the node-averaged flux shape in selected assemblies. Marker placement corresponds to the location of the node centre. Numbering corresponds to the assemblies along the radius at an angle of 60 degrees from the positive x-axis in Fig. 3.

spatial and spectral distortion of the neutron population, therefore testing the performance of quasi-statics to follow these modifications. Test cases of this nature have been extensively used in the literature in the development and testing of quasi-static algorithms (Yasinsky and Henry, 1965). In the present situation, the distributions in Figs. 4 and 5 of the asymptotic configuration of the system are more or less reflected through $z/H = 1/2$, though not exactly as the system is not perfectly symmetric due to the material pattern of the central assembly.

4.1. Study of the performance of the quasi-static schemes

The transient is modelled using each of the available quasi-static methods. Relative convergence criteria of 10^{-10} are imposed on the effective multiplication eigenvalue of the initial system and 10^{-8} on the L_2 norm of the flux at each inversion of the problem. Quasi-static computations are performed with constant shape time steps employing a reactivity time step of 10^{-5} s and one amplitude time step per reactivity time step, solving exactly the amplitude equations across the reactivity time step. For calculations which use IQM or IIQM, the normalisation condition iterations are stopped if the relative change in the γ value (see Eq. (7)) falls below 10^{-6} or after a maximum of three normalisation condition iterations.

The time-dependent behaviour of the normalised total power computed with the quasi-static methods is presented in Fig. 6, where the reference solution is the result of a full inversion of the problem using a fully implicit integration scheme on a fine discretisation of the time domain ($\Delta t_\varphi = 10^{-6}$ s). These results demonstrate the typical features of the quasi-static approaches. In IQM, the shape at the beginning of the shape time step is projected forward, resulting in

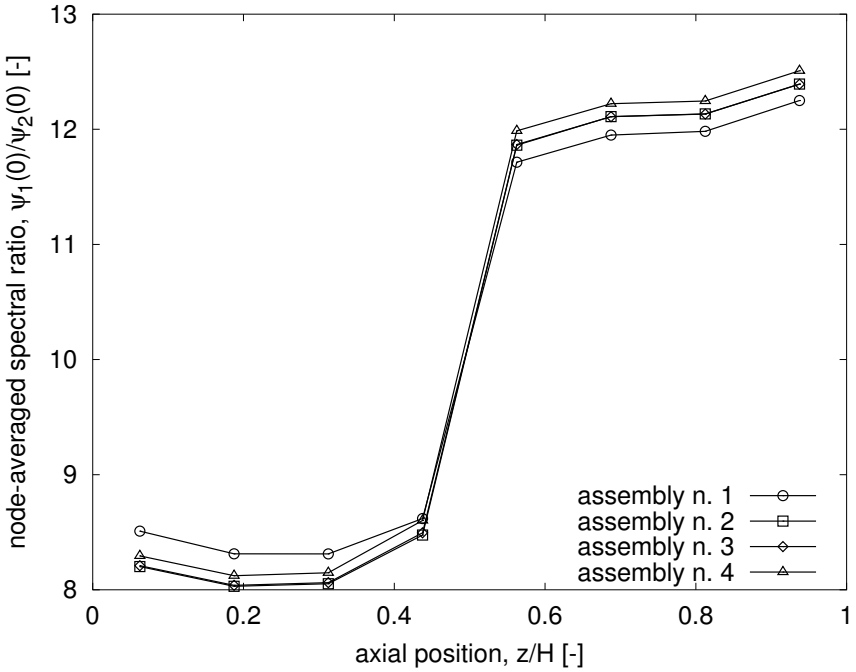

Figure 5: Initial axial distribution of the node-averaged spectral ratio in selected assemblies. Marker placement corresponds to the location of the node centre. Numbering corresponds to the assemblies along the radius at an angle of 60 degrees from the positive x-axis in Fig. 3.

an evolution of the power which is identical to that of the PK solution up to the time at which the shape is updated. At this same point in time, a discontinuity of the first derivative of the power is introduced by the normalisation condition iterations. Instead, in IIQM and PCQM, the availability of the shape function at the end of the shape time step, together with its use in the approximation of the behaviour of the shape within the shape time step by something other than a constant, results in an evolution which begins to diverge from the PK solution from the very start. The similarity of the results produced by IIQM and PCQM is as expected, as both methods, although by different algorithms, employ the same equations and the same approximations to describe the power.

The time-dependent behaviours of the integral kinetics parameters are presented in Figs. 7, 8 and 9 for the various methods of solution and the various discretisations of the time domain. In each case, the reference value is obtained by employing the normalised reference solution in the appropriate definition. For each of the dynamic reactivity, Fig. 7, the neutron lifetime, Fig. 8, and the effective delayed neutron fraction, Fig. 9, it is observed that the ability to approximate the reference value is enhanced through the approximation of the shape function as being linear across the shape time step. In comparing the results of IIQM and those of PCQM, it can be noted that PCQM computes visibly better results, especially at large time steps, for precisely the reason that satisfaction of the normalisation condition is automatically guaranteed. From Fig. 7, one can observe that the reactivity after 250 reference lifetimes is not zero; in fact, the new asymptotic steady-state condition is reached only when

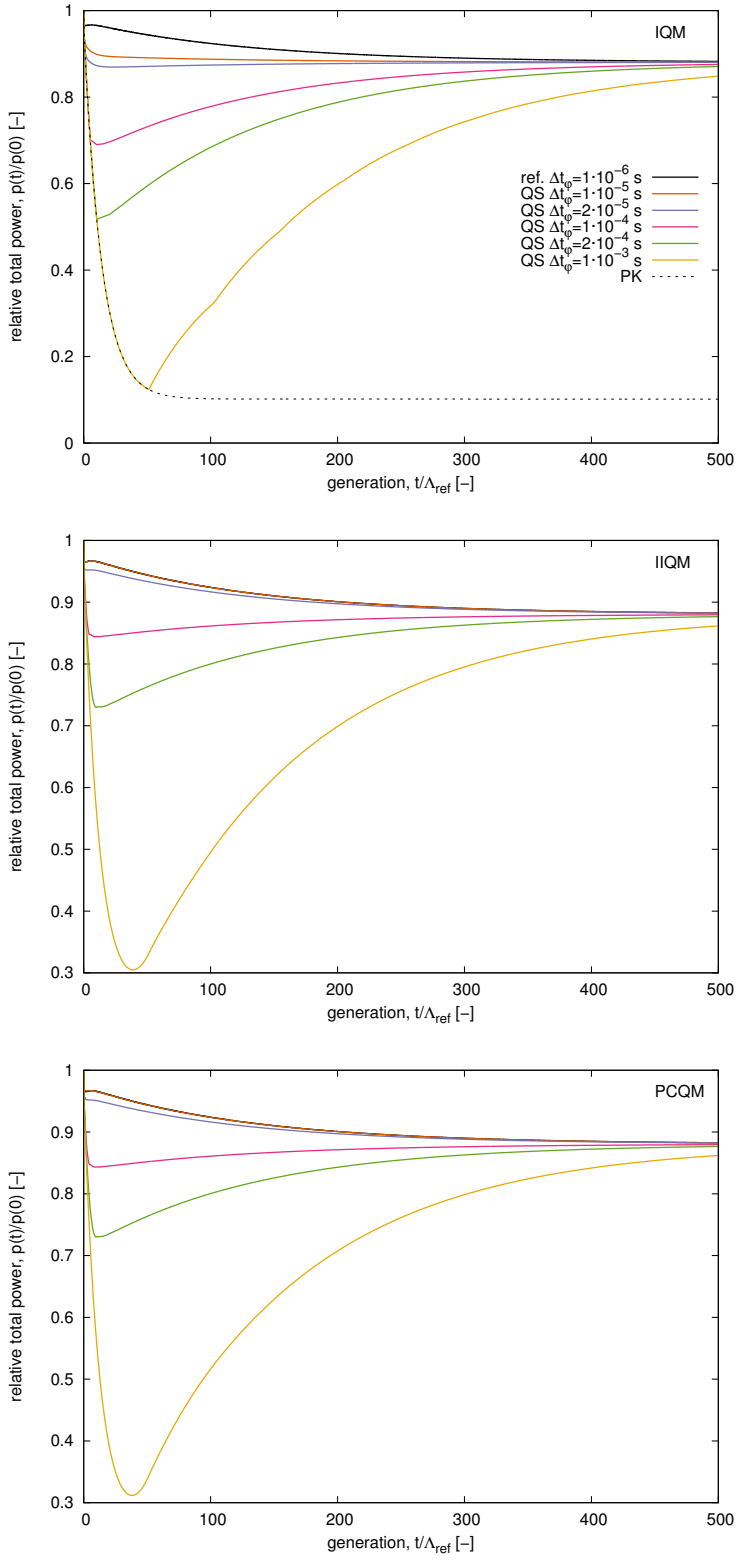

Figure 6: Time-dependent behaviour of the total power for the compensated transient ($\Lambda_{ref} = 1.94724 \cdot 10^{-5}$ s).

full equilibrium between neutrons and precursors is established, which happens later in time.

In Figs. 10 and 11, the time-dependent behaviours of the amplitude and the effective delayed neutron precursor amplitude are reported. The discontinuities which are present for both the amplitude (IQM) and the effective delayed neutron precursor amplitude (IQM and IIQM) are a consequence of the different algorithmic methodologies. In IQM, the unavailability of the shape at the end of the shape time step, hence the inability to apply the approximations that the power density per unit amplitude and the fission source density per unit amplitude vary continuously across the shape time step, inevitably lead to discontinuities of the effective quantities if the continuity of the physical quantities is to be enforced at the interfaces of a shape time step over which the shape has significantly varied. Instead, both IIQM and PCQM have access to the shape at the end of the shape time step, thereby permitting the assumption of a continuous variation of the physical quantities across the shape time step and therefore leading to the contemporaneous, continuous evolution of both the effective and the physical quantities, or at least would do so if normalisation was satisfied. Figure 10 shows that the amplitude is not approaching asymptotically the initial unitary value, because the space-energy transient induced by the material modification is causing a change in the total number of neutrons that affects the final steady-state of the system. This is also the reason for which the power level, as can be seen in Fig. 6, is changing between the two critical steady-states.

The error of the quasi-static methods is a time-dependent quantity in virtue of the manner in which the method accounts for the time-dependence of the flux and the manner in which the method both resolves and accounts for the phenomena that occur within the various levels of the multiscale discretisation of the time domain. This is demonstrated, for example, by examining the temporal evolution of the relative error of the total power with respect to the reference solution, as shown in Fig. 12. For a fixed temporal discretisation, all methods exhibit two distinct regions: one in which the error is greater and possibly a function of time and one in which it is notably less and approximately constant. The former results from the ability of the quasi-static method to accurately solve for the shape, and consequently all of the derived quantities, during parts of the transient characterised by the evolution of the spatial and/or spectral distributions. Naturally, the error is controlled only when the discretisation sufficiently resolves these variations. As the spatial and/or spectral effects become less prominent, the shape can be computed with increasing accuracy, causing the global error to decrease and ultimately leading to the latter region, the residual of which characterises the error accumulated during the spatial and/or spectral transient.

As regards a comparison among the methods, IIQM and PCQM are characterised by a lower error than IQM for a given shape time step thanks to the use of the shape function at the end time step over which the integration is performed. All methods regularly decrease the error in all parts of the transient as the shape time step is decreased; however, IIQM and PCQM exhibit convergence rates which are more favourable than that of IQM. The irregular behaviour seen for the finest discretisations in the calculations which use IIQM and PCQM are attributed to numerical noise caused by the magnitude of the error of the temporal discretisation and, in the case of IIQM, that of the normalisation condition, approaching the magnitude of the global error of the

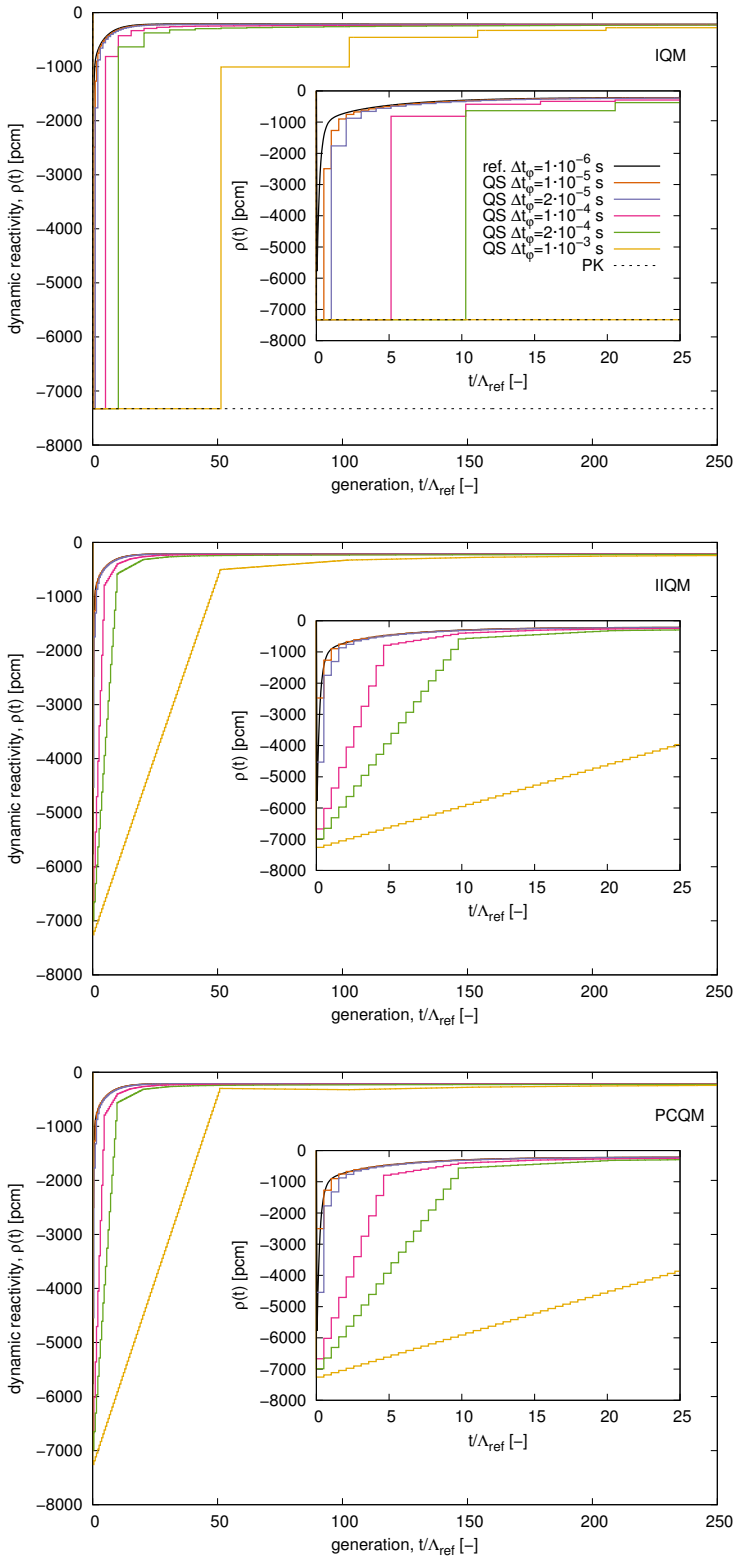

Figure 7: Time-dependent behaviour of the dynamic reactivity for the compensated transient ($\Lambda_{ref} = 1.94724 \cdot 10^{-5}$ s).

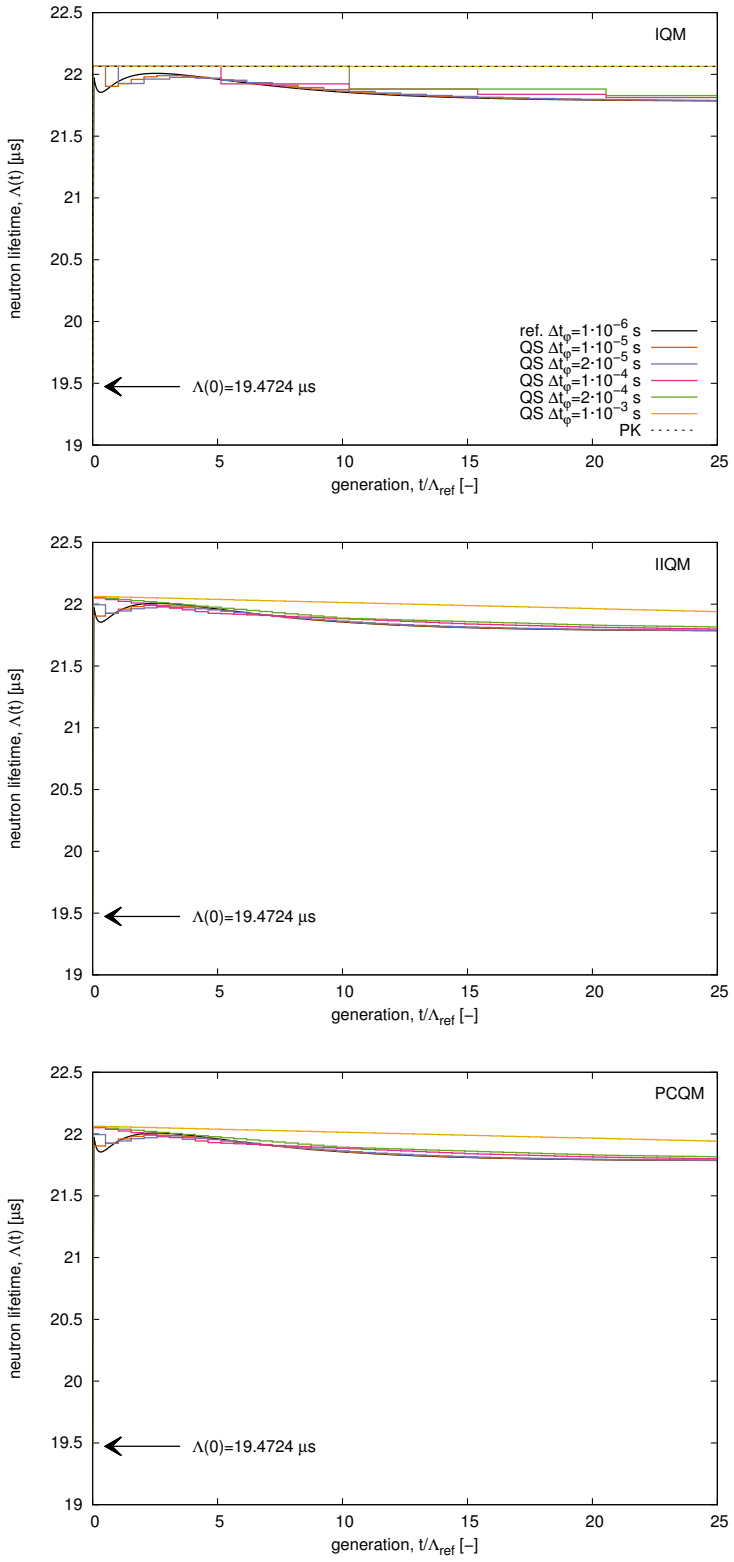

Figure 8: Time-dependent behaviour of the neutron lifetime for the compensated transient ($\Lambda_{ref} = 1.94724 \cdot 10^{-5}$ s).

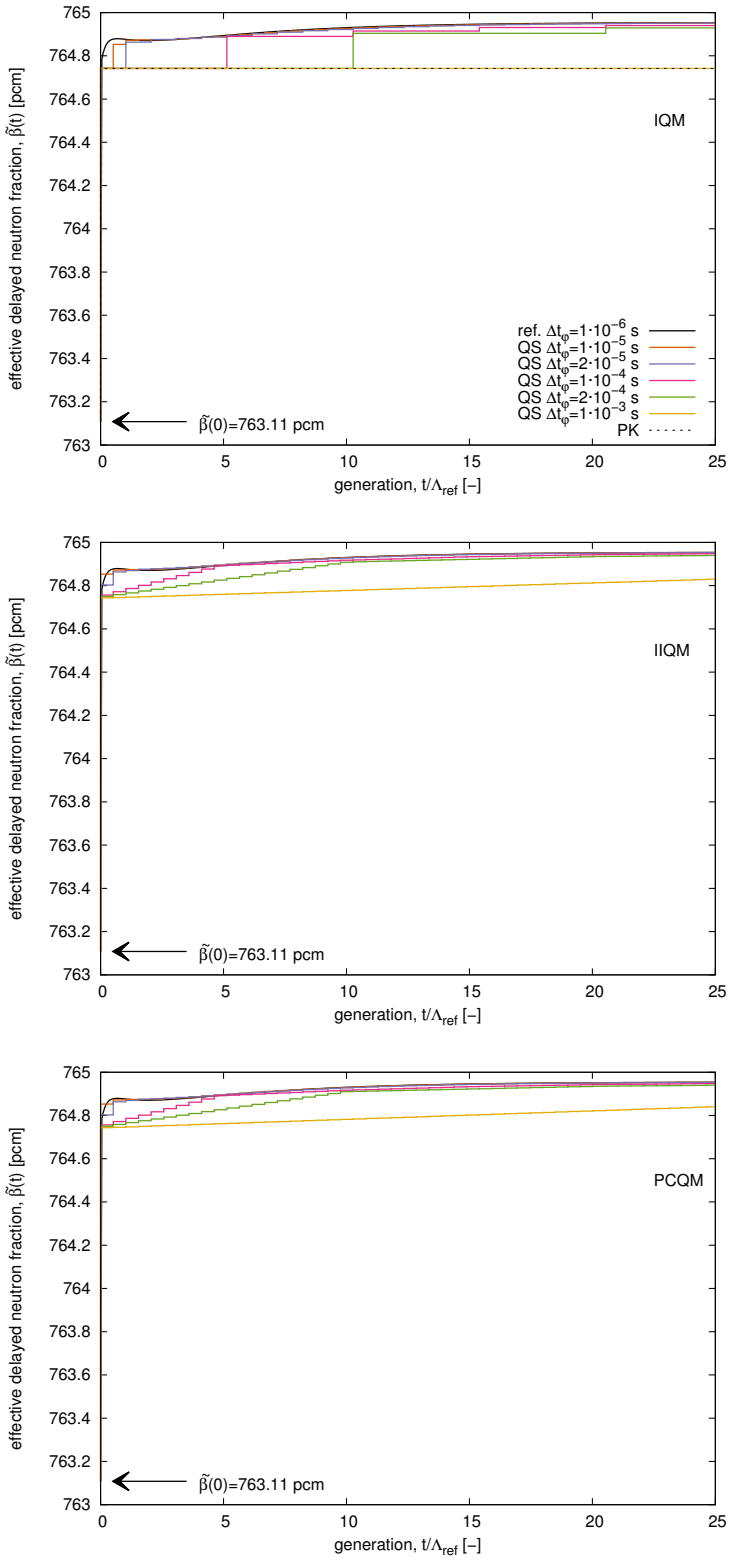

Figure 9: Time-dependent behaviour of the effective delayed neutron fraction for the compensated transient ($\Lambda_{ref} = 1.94724 \cdot 10^{-5}$ s).

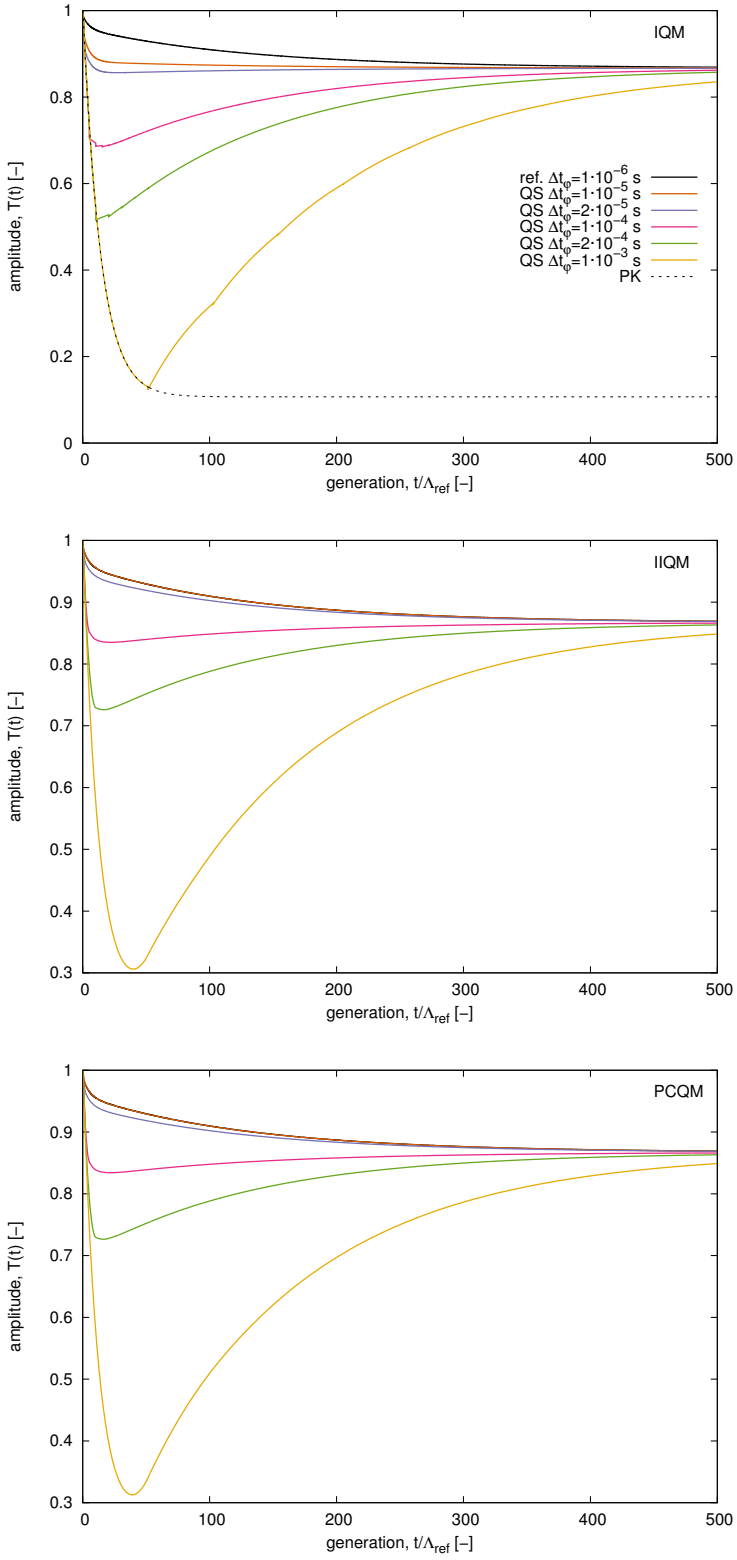

Figure 10: Time-dependent behaviour of the amplitude for the compensated transient ($\Lambda_{ref} = 1.94724 \cdot 10^{-5}$ s).

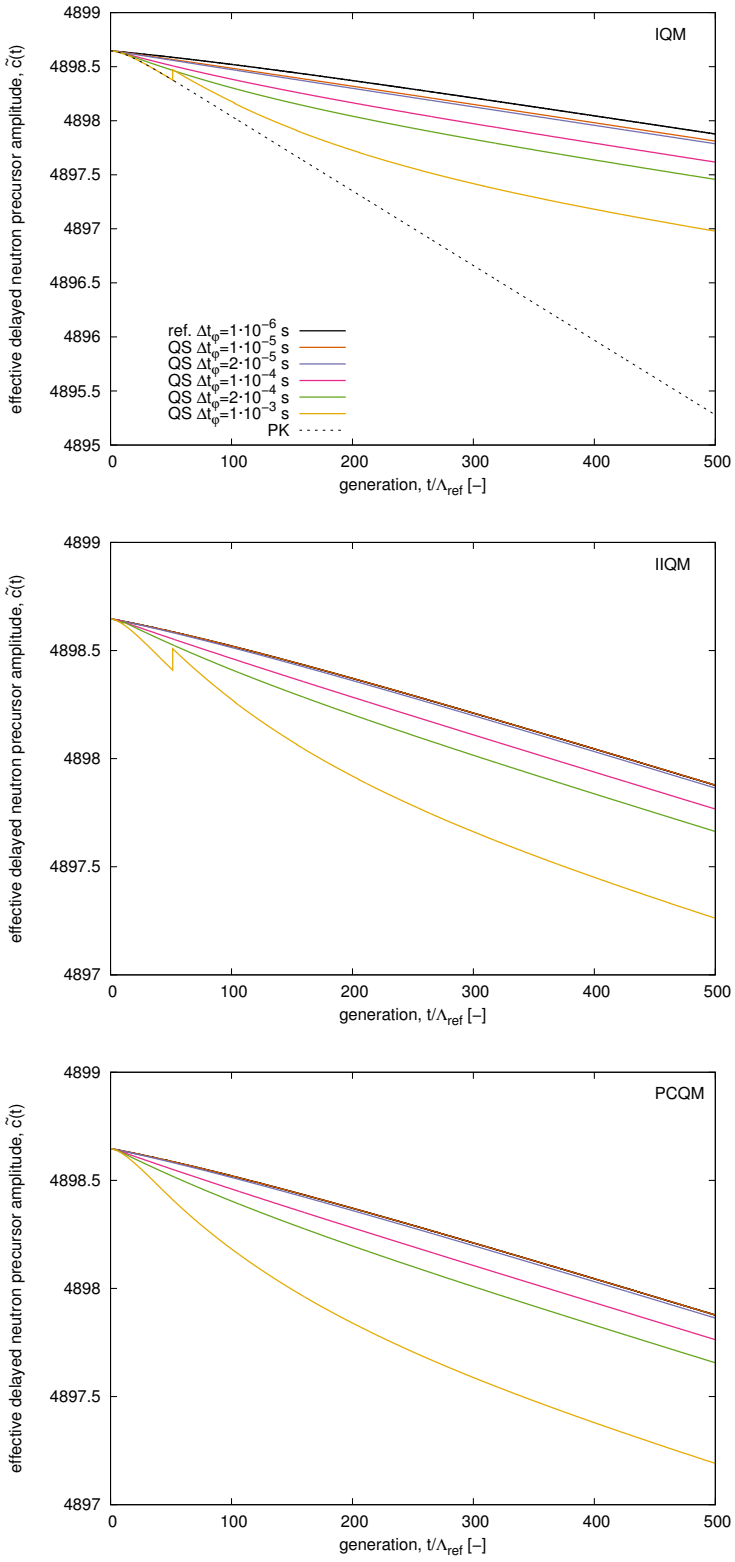

Figure 11: Time-dependent behaviour of the effective delayed neutron precursor amplitude for the compensated transient ($\Lambda_{ref} = 1.94724 \cdot 10^{-5}$ s).

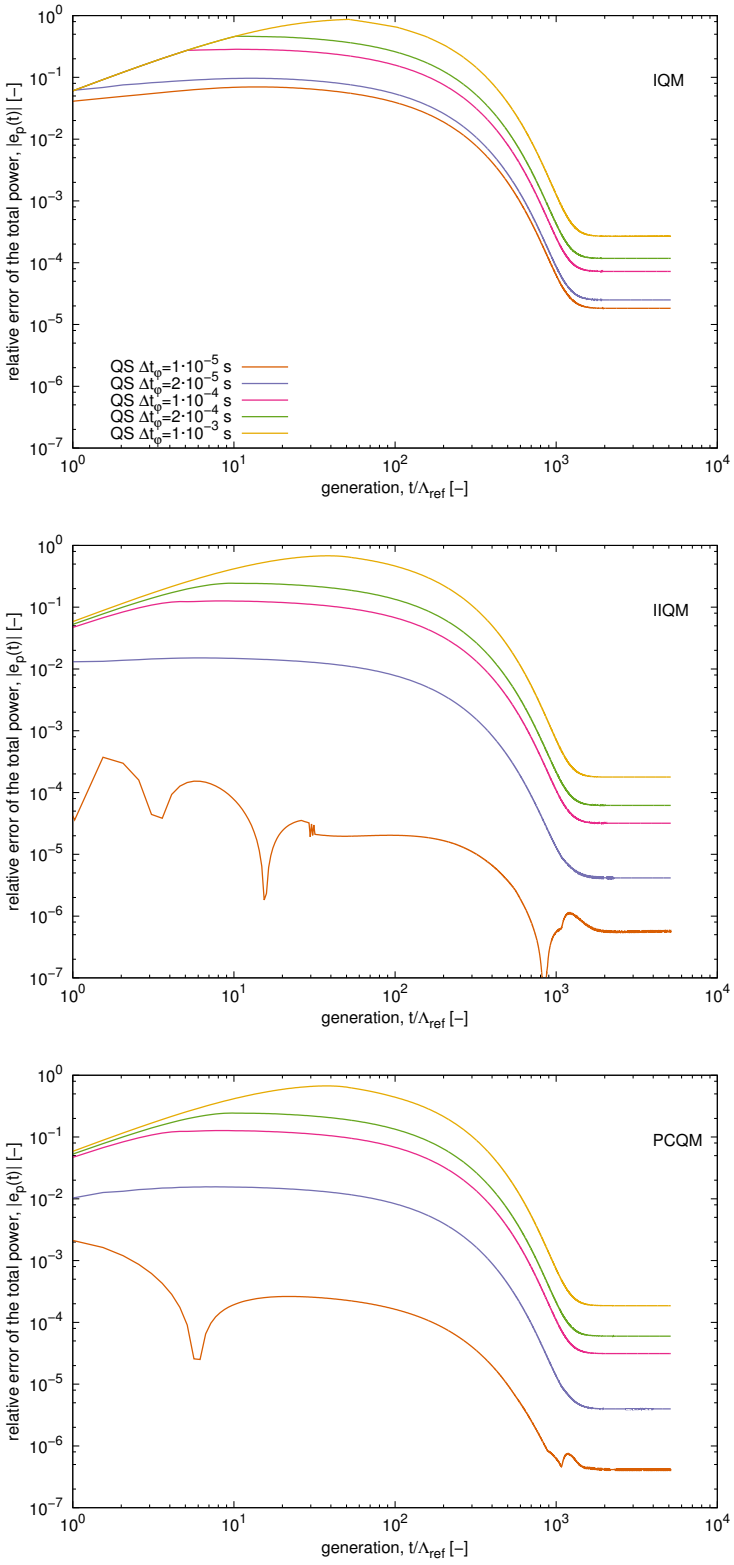

Figure 12: Time-dependent behaviour of the relative error of the total power for the compensated transient ($\Lambda_{ref} = 1.94724 \cdot 10^{-5}$ s).

solution.

Some insight into the last point is obtained by examining the behaviour of the normalisation condition error in parallel with that of the power. The time-dependent behaviour of the normalisation condition error is shown in Fig. 13 for both IQM and IIQM, indicating also the number of normalisation condition iterations performed at each discrete point in time. For a fixed number of normalisation condition iterations, the normalisation condition error decreases as the spatial and/or spectral effects of the transient disappear, ultimately becoming such that the convergence criterion imposed on the normalisation condition error can be satisfied in fewer iterations and, accordingly, the iterative algorithm terminates sooner. However, this can produce drastic jumps of the accepted normalisation condition error between successive shape computations, which in turn can lead to the oscillatory behaviour observed in Fig. 12 when the normalisation condition error becomes the dominant source of the error.

Another set of observations regarding Fig. 13 may be made in reference to the relative values of the normalisation error between IQM and IIQM. Namely, when multiple normalisation condition iterations occur, it appears that the normalisation error of IQM tends to be less than that of IIQM. This is justified by recalling the different iterative methodologies, with particular reference to the fact that in the normalisation conditions of IIQM with respect to those of IQM, more quantities are computed implicitly on the basis of the shape at the end of the shape time step, thus causing an amplification of any variation which occurs from normalisation iteration to normalisation iteration. Despite this apparent drawback of IIQM in comparison to IQM, at least in the present example, the normalisation condition error does not lead to a situation in which IIQM produces results which are worse than those of IQM.

A final, overall assessment of the accuracy of the computed solution and the computational efficiency of the methods is presented in Table 2. The comparison is made at 10^{-1} s, after the error has stabilised for the solution computed by all methods. As regards accuracy, it is again observed that IIQM and PCQM are superior to IQM both in terms of the accuracy itself and the rate of convergence. Moreover, for both IIQM and PCQM, the quasi-static solutions computed with the finest discretisation of the time domain differ from the reference solution, which is computed with a time step that is an order of magnitude less, only in the last significant digit.

In terms of performance, PCQM is able to perform fewer inversions of the flux equations than IQM is required to perform of the shape equations due to the necessity to satisfy the normalisation condition. However, for a shape time step which is sufficiently small so as to decrease the number of normalisation condition iterations, the total number of outer iterations may be less for IQM than for PCQM in virtue of the fact that in solving for the shape, possible amplitude effects are not present. This benefit decreases as the shape time step is increased, namely due to the fact that the number of normalisation condition iterations per shape time step tends to increase. The technique employed by MPCQM can significantly reduce the number of outer iterations for sufficiently small shape time steps in comparison to PCQM, rendering the method comparable to IQM in terms of the number of outer iterations. Again, the benefit depends on the shape time step and decreases, possibly even becoming detrimental, as the shape time step is increased due to the lower probability to predict the correct amplitude at the end of the shape time step. The required

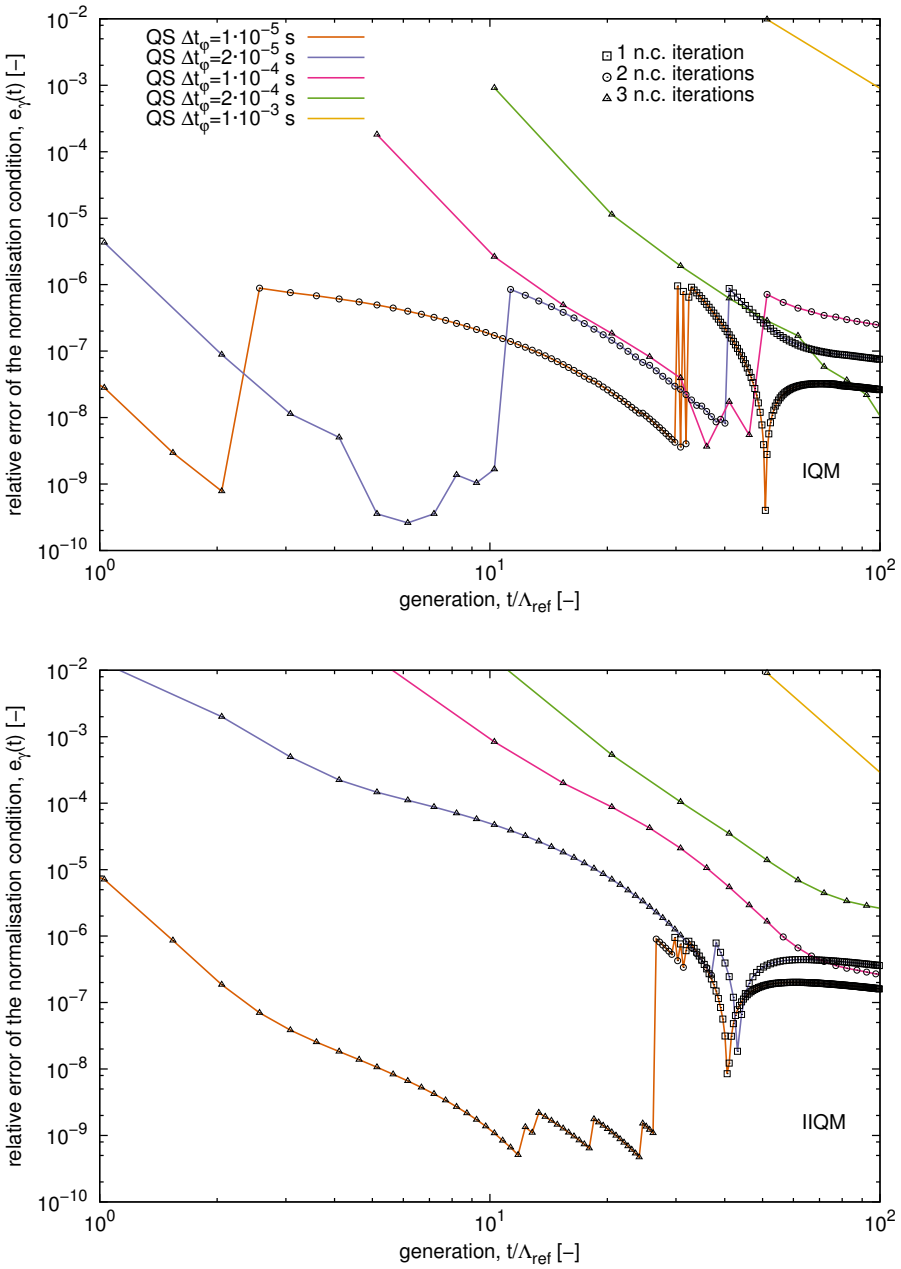

Figure 13: Time-dependent behaviour of the normalisation condition (n.c.) error for the compensated transient ($\Lambda_{ref} = 1.94724 \cdot 10^{-5}$ s).

number of inversions of the shape equations and the number of outer iterations of IIQM are more or less comparable to those of IQM; however, as IIQM performs the integration of the amplitude equations as part of the normalisation condition iterations, the computational time required is slightly greater. This hardly seems pertinent in light of the discussion of the accuracy of IIQM with respect to that of IQM.

Table 2: Comparison of the performance and the quality of the computed solution for the quasi-static algorithms (evaluation at 10^{-1} s).

	IQM					IIQM				
Δt_φ [s]	NI	NO	e_ϕ^2 [-]	e_p^2 [-]	e_p^∞ [-]	NI	NO	e_ϕ^2 [-]	e_p^2 [-]	e_p^∞ [-]
1.00e-05	10065	19146	1.83e-05	1.83e-05	1.83e-05	10111	21719	5.61e-07	5.79e-07	5.70e-07
2.00e-05	5050	17207	2.49e-05	2.51e-05	2.50e-05	5067	18035	4.14e-06	4.18e-06	4.15e-06
1.00e-04	1116	12166	7.21e-05	7.25e-05	7.22e-05	1073	10877	3.18e-05	3.21e-05	3.19e-05
2.00e-04	607	9474	1.17e-04	1.18e-04	1.17e-04	588	8579	6.17e-05	6.22e-05	6.19e-05
1.00e-03	221	6800	2.68e-04	2.70e-04	2.69e-04	215	6495	1.78e-04	1.79e-04	1.78e-04

	PCQM					MPCQM				
Δt_φ [s]	NI	NO	e_ϕ^2 [-]	e_p^2 [-]	e_p^∞ [-]	NI	NO	e_ϕ^2 [-]	e_p^2 [-]	e_p^∞ [-]
1.00e-05	10001	27095	4.11e-07	4.18e-07	4.13e-07	10001	19723	4.53e-07	4.59e-07	4.53e-07
2.00e-05	5001	20967	3.96e-06	3.99e-06	3.97e-06	5001	16801	4.02e-06	4.04e-06	4.02e-06
1.00e-04	1001	6960	3.12e-05	3.13e-05	3.12e-05	1001	7837	3.12e-05	3.13e-05	3.12e-05
2.00e-04	501	5793	5.98e-05	6.01e-05	5.99e-05	501	6684	5.98e-05	6.00e-05	5.98e-05
1.00e-03	101	2420	1.86e-04	1.87e-04	1.86e-04	101	2980	1.86e-04	1.87e-04	1.86e-04

NI: total number of inversions of the flux or shape equations performed up to the point of evaluation; NO: total number of outer iterations performed up to the point of evaluation; e_ϕ^2: L_2 norm of the flux distribution; e_p^2: L_2 norm of the power distribution; e_p^∞: L_∞ norm of the total power.

4.2. Study of the adaptive time integration procedure

The points evidenced in the preceding discussion support the idea that an adaptive time integration procedure is the natural complement of a quasi-static method. In comparing the results of the quasi-static computations using constant shape time steps, it is observed that the quality of the results propagated throughout the transient depends on how well resolved are the most onerous parts of the transient. The introduction of an algorithm which is capable of an adaptive handling (either refining of coarsening, as may be required) of the shape time step can simultaneously provide better resolution of the most difficult portions of the transient and eliminate superfluous computations of the shape as the system tends to an asymptotic configuration.

In this context, the behaviour of the relative distortion of the shape function, $\xi_\psi(t)$, for the transient under consideration is introduced in Fig. 14. For brevity, only the results of the solution computed by the full inversion method are shown; results obtained by the quasi-static methods which use constant shape time steps exhibit similar behaviour. Regardless of the value of the shape time step, the general behaviour of the relative distortion is analogous. As the spatial and/or spectral effects diminish, the distortion decreases and ultimately tends to a constant value which may be accompanied by numerical noise. The magnitude of the distortion at any point in time depends on that which has occurred in the preceding time step. Thus, at equal points in time, the magnitude of the distortion decreases with decreasing shape time step.

The results for two weighting procedures are shown: one which equally weights all points of the phase space and one which weights on the adjoint solution of the initial configuration. For this particular transient, the results are not strongly affected by the two choices of the weight function; however, the adjoint-weighted distortion is consistently less than the unit-weighted distortion. This behaviour is not universal, but rather problem dependent. Henceforth, when reference is made to the distortion of the shape function, the adjoint weighting procedure is implied.

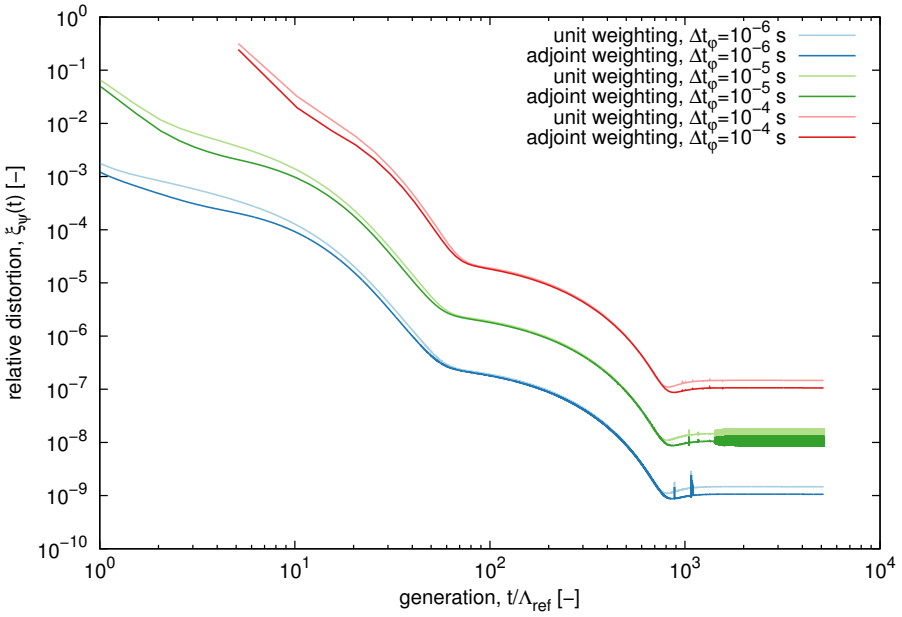

Figure 14: Time-dependent behaviour of the relative distortion of the shape function for the full inversion method ($\Lambda_{ref} = 1.94724 \cdot 10^{-5}$ s).

The same transient is modelled again using the quasi-static methods with the adaptive integration procedure enabled. Convergence criteria are as before and the integration parameters are fixed at a maximum shape time step of 10^{-1} s and a maximum reactivity time step of 10^{-2} s.

A comparison of the asymptotic solution computed by the various quasi-static algorithms using the adaptive integration procedure is presented in Table 3. It is observed that each of the individual methods exhibits convergence for a maximum permissible distortion less than 10^{-2} and that in allowing the permitted distortion to increase to 10^{-1}, the effect on the solution is minimal. The latter observation implies that the starting procedure of the algorithm and the maximum multiple by which the shape time step is allowed to expand between successive shape time steps are relatively conservative. As concerns a comparison of the methods, IQM and IIQM reach the asymptotic state at approximately the same time, which is slightly later than that of PCQM, and IQM yields results which are different than those of IIQM and PCQM, both of which are nearly the same. As in the case of a constant shape time step, IQM and IIQM do give different results due to their different treatment of the physical

quantities during the normalisation iterations, while IIQM and PCQM yield identical results provided that the normalisation error is sufficiently small. In the present case, the additional difference between IIQM and PCQM may be attributed to the different means by which the shape time step is managed for the two methods, namely that IIQM applies additional constraints which ultimately lead to a slower rate of expansion of the shape time step and, consequently, a better resolution of the time domain in the vicinity of the perturbation.

Comments which may be made on the performance are dependent on the method. Considering first PCQM and MPCQM, both the number of times the flux equations are inverted and the number of outer iterations monotonically increase with an increasingly stringent limit on the maximum permissible distortion, but the ratio of the number of outer iterations to the number of inversions decreases, all of which is as to be expected. While PCQM and MPCQM employ the same number of inversions of the flux equations, the number of outer iterations for MPCQM is greater than that for PCQM in this particular transient. This is a consequence of the fact that for a compensated transient, the most significant changes are to the shape rather than to the amplitude; therefore, the potential benefits offered by MPCQM do not necessarily come into effect. Considering next IQM and IIQM, the performance behaviour is more disordered due to the non-linearities of these two quasi-static algorithms and due to the additional constraints imposed by the adaptive integration procedure in the management of the shape time step, making any general observation difficult. Regarding a comparison between IQM and IIQM, IIQM requires both a greater number of inversions of the shape equations and a greater number of outer iterations than IQM, but the number of outer iterations per inversion is less. This is related to normalisation requirements through the error reduction behaviour of the normalisation condition error and, therefore, to the adaptive integration procedure.

Table 3: Comparison of the performance and the quality of the computed solution for the quasi-static algorithms (evaluation at the asymptotic state).

	IQM				IIQM			
$\xi_\psi^{\max}$ [-]	t^* [s]	$p(t^*)/p(0)$ [-]	NI	NO	t^* [s]	$p(t^*)/p(0)$ [-]	NI	NO
1.00e-03	1.7417e+02	8.7813e-01	8541	310402	1.7415e+02	8.7890e-01	29148	901599
1.00e-02	1.7391e+02	8.7813e-01	9163	341764	1.7392e+02	8.7889e-01	39540	1020065
1.00e-01	1.7385e+02	8.7810e-01	7195	283304	1.7392e+02	8.7889e-01	36476	1014204

	PCQM				MPCQM			
$\xi_\psi^{\max}$ [-]	t^* [s]	$p(t^*)/p(0)$ [-]	NI	NO	t^* [s]	$p(t^*)/p(0)$ [-]	NI	NO
1.00e-03	1.6853e+02	8.7889e-01	2012	29955	1.6853e+02	8.7889e-01	2012	63683
1.00e-02	1.6859e+02	8.7889e-01	1730	28466	1.6855e+02	8.7889e-01	1730	62356
1.00e-01	1.6861e+02	8.7888e-01	1704	28368	1.6856e+02	8.7888e-01	1703	62164

t^*: time at which asymptotic state is reached, determined through the application of a least squares fit to the logarithm of the power evolution and the identification of the earliest time for which the fit satisfies all downstream values with a norm of the residual less than 10^{-7}; NI: total number of inversions of the flux or shape equations performed up to t^*; NO: total number of outer iterations performed up to t^*.

Instead, a more insightful approach may be to consider also the employed shape time step, as is shown in Fig. 15. In the case of the linear approach used by PCQM and in the absence of other factors, the shape time step expands

proportionally to the minimum of the ratio of the maximum permissible distortion to the distortion at the current shape time step or the maximum allowable rate of expansion until it reaches its maximum absolute value. However, in the non-linear cases of IQM and IIQM, the expansion of the shape time step is furthermore limited by considerations on the normalisation requirement. In the present algorithm, this implies further decreasing the rate of expansion (possibly to zero) on the basis of the normalisation condition error at the previous shape time step, which results in the additional plateaus at shape time steps which are less than the maximum absolute value. In all cases, the occasional instantaneous drops in the shape time step are attributed to the algorithm adjusting itself so as to generate output at a specific point in time requested by the user.

In conclusion to this study on the adaptive integration procedure, it is worth noting that a single parameter study is not completely representative of the situation. There are several parameters which are evaluated by the time step selection algorithm, of which the relative distortion of the shape function is only one. Consequently, a completely consistent basis for comparison among the methods is difficult to ensure.

Results obtained with the application of the adaptive algorithm are presented only in the absence of thermal feedback. Since the time step adaptation is based on the rate of change of the neutron shape, the presence of thermal feedback and the consequent modification of the shape should not influence the application of the algorithm.

5. Conclusions

A quasi-static solver for the solution of the time-dependent neutron diffusion equations is implemented in the neutronics module of a multiphysics reactor analysis code. The paper includes an introductory critical review of the quasi-static scheme, illustrating the classic formulation as well as the novel modifications recently proposed to overcome some of the drawbacks of the original method. The various formulations of the method are then applied within a three-dimensional spatial nodal discretisation scheme in hexagonal-z geometry for the multigroup diffusion model for nuclear reactor kinetics applications.

Results and comparisons of some transient test calculations clearly demonstrate the characteristics of the different quasi-static approaches, highlighting advantages and problems that may arise in their application. It is also realised that the quasi-static scheme can be efficiently used only in connection to a consistent procedure to adapt the time step between shape recalculations according to the evolution of the neutron distribution within a system in a specific transient. The paper proposes a novel adaptive time stepping algorithm that is shown to be potentially capable to significantly improve the effectiveness of the quasi-static procedure for realistic transient calculations.

Acknowledgement

This work is carried out under the auspices and with the financial support of 'Accordo di Programma Ministero dello Sviluppo Economico - ENEA sulla Ricerca di Sistema Elettrico' and of CIRTEN (Consorzio Interuniversitario per la Ricerca Tecnologica Nucleare).

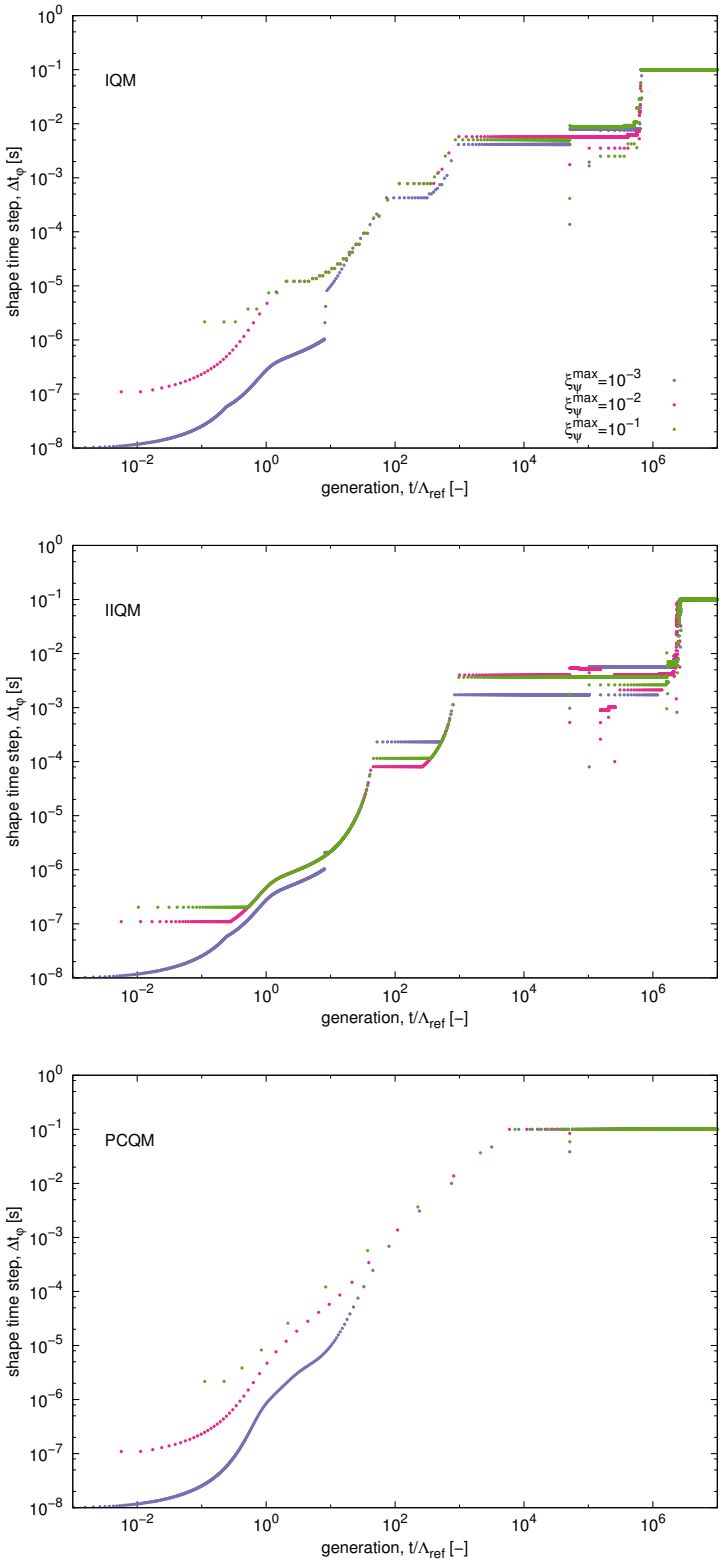

Figure 15: Time-dependent behaviour of the shape time step ($\Lambda_{ref} = 1.94724 \cdot 10^{-5}$ s).

References

Bonifetto, R., Caron, D., Dulla, S., Ravetto, P., Savoldi Richard, L., Zanino, R., 2013a. Extension of the FRENETIC code capabilities to the 3D neutronic/thermal-hydraulic dynamic simulation of lead-cooled fast reactors. In: 16th International conference on emerging nuclear energy systems (ICENES 2013). Madrid, 26-30 May 2013.

Bonifetto, R., Dulla, S., Ravetto, P., Savoldi Richard, L., Zanino, R., 2013b. A full-core coupled neutronic/thermal-hydraulic code for the modeling of lead-cooled nuclear fast reactors. Nuclear Engineering and Design 261, 85–94.

Devooght, J., Mund, E., 1980. Generalized quasi-static method for nuclear reactor space-time kinetics. Nuclear Science and Engineering 76, 10–17.

Dulla, S., Cadinu, F., Picca, P., Ravetto, P., 2006. Effects of neutron source characteristics in direct and adjoint problems for subcritical systems. International Journal of Nuclear Energy Science and Technology 2 (4), 361–377.

Dulla, S., Mund, E. H., Ravetto, P., 2008. The quasi-static method revisited. Progress in Nuclear Energy 50, 908–920.

Henry, A. F., 1958. The application of reactor kinetics to the analysis of experiments. Nuclear Science and Engineering 3, 52–70.

Kao, P. W., Henry, A. F., 1989. Supernodal analysis of PWR transients. In: Hall, M. (Ed.), Proceedings of the Topical meeting on advances in nuclear engineering computation and radiation shielding. American Nuclear Society, p. 63, Santa Fe, New Mexico, 9-13 April 1989.

Lawrence, R. D., 1983. The DIF3D nodal neutronics option for two- and three-dimensional diffusion-theory calculations in hexagonal geometry. Tech. Rep. ANL-83-1, Argonne National Laboratory.

Lewins, J., 1965. Importance, the adjoint function: the physical basis of variational and perturbation theory in transport and diffusion problems. Pergamon, Oxford.

Meneley, D. A., Ott, K. O., Wiener, E. S., 1967. Space-time kinetics - the QX1 code. Tech. Rep. ANL-7310, Argonne National Laboratory.

Ott, K. O., Madell, J. T., 1966. Quasistatic treatment of spatial phenomena in reactor dynamics. Nuclear Science and Engineering 26, 563–565.

Ott, K. O., Meneley, D. A., 1969. Accuracy of the quasistatic treatment of spatial reactor kinetics. Nuclear Science and Engineering 36, 402–411.

Shober, R. A., Daly, T. A., Ferguson, D. R., 1978. FX2-TH: A two-dimensional nuclear reactor kinetics code with thermal-hydraulic feedback. Tech. Rep. ANL-78-97, Argonne National Laboratory.

Ussachoff, L. N., 1956. Equation for the importance of neutrons, reactor kinetics and the theory of perturbation. In: Proceedings of the international conference on the peaceful uses of atomic energy. Vol. V. United Nations, pp. 503–510, Geneva, 8-20 August 1955.

Wigner, E. P., 1992. Effect of small perturbations on pile period. In: Weinberg, A. M. (Ed.), The collected works of Eugene Paul Wigner, Part A: The scientific papers, Vol. 5: Nuclear energy. Springer, Berlin, pp. 540–552.

Yasinsky, J. B., Henry, A. F., 1965. Some numerical experiments concerning space-time reactor kinetics behavior. Nuclear Science and Engineering 22, 171–181.